BENJAMIN A. MOSLEY

COMBINED EFFECTS OF TURBULENCE AND NUTRIENT ENRICHMENT ON COMPETITION DYNAMICS BETWEEN DIATOMS AND HETEROTROPHIC BACTERIA

UNIVERSIDADE DO ALGARVE

FACULDADE DE CIÊNCIAS E TECNOLOGIA

2020

BENJAMIN A. MOSLEY

COMBINED EFFECTS OF TURBULENCE AND NUTRIENT ENRICHMENT ON COMPETITION DYNAMICS BETWEEN DIATOMS AND HETEROTROPHIC BACTERIA

MASTERS IN MARINE AND COASTAL SYSTEMS

WORK PERFORMED UNDER THE SUPERVISION OF:

PROFESSOR HELENA GALVÃO (UNIVERSIDADE DO ALGARVE, CIMA)

DR PEDRO CERMEÑO (INSTITUTO DE CIENCIAS DEL MAR, BARCELONA)

UNIVERSIDADE DO ALGARVE

FACULDADE DE CIÊNCIAS E TECNOLOGIA

2020

DECLARAÇÃO DE AUTORIA DE TRABALHO / DECLARATION OF AUTHORSHIP OF WORK

Declaro ser o(a) autor(a) deste trabalho, que é original e inédito. Autores e trabalhos consultados estão devidamente citados no texto e constam da listagem de referências incluída.

I declare to be the author of this work, which is original and unpublished. Authors and works consulted are duly cited in the text and are included in the list of references.

X 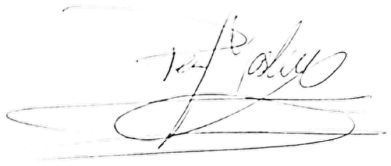

Benjamin A. Mosley

ABSTRACT

Time series data of Chlorophyll a, dissolved organic carbon, heterotrophic bacteria and autotrophic biomass obtained from incubations of water samples collected 1 km south from El Masnou, (Mediterranean Sea) were analysed. This was used to explore the competitive dynamics of heterotrophic bacteria and diatoms under different environmental conditions and to investigate the influence of turbulence. Eight microcosm experiments were set up with daily addition of nitrogen and phosphorus at Redfield ratios. Groups of containers were enriched or depleted in silicate and glucose. Four of the microcosms were subject to artificial turbulence. The microcosm set-ups were glucose; glucose and silicate; glucose, silicate and turbulence; glucose and turbulence; turbulence only; silicate only; silicate and turbulence; and a control with no addition of silicate or glucose and no turbulence. It was found that turbulence had no influence on the competition between heterotrophic bacteria and diatoms however there was a difference based on the varying silicate or glucose environments. As was to be expected, the bacterial biomass increased rapidly in the microcosms with added glucose. Following this was an increase in autotrophic biomass, particularly when silicate was present, and a subsequent decrease in bacterial biomass, indicating a high level of grazing. In the absence of glucose, the bacteria did not grow as rapidly in the microcosm containing silicate, and there was little change in biomass in the container without silicate. The autotroph numbers increased in the silicate replete microcosm before declining. In the set-up without glucose or silicate, the biomass dropped initially which was expected but then increased. This increase was attributed to bacterial remineralisation of dissolved organic

carbon sources, presumably derived from protozoans, flagellates and ciliates. This subsequent remineralisation may have had an impact on diatom growth and reproduction. Turbulence had no significant effect on phytoplankton competition which may highlight a limitation to microcosm experiments.

Key words: Diatoms; Heterotrophic Bacteria; Phytoplankton Competition; Turbulence; Microbial food-web

RESUMO

O presente estudo teve como objetivo expandir trabalhos anteriores que investigaram a dinâmica competitiva entre diatomáceas e bactérias heterotróficas. Num sistema oligotrófico estratificado, bactérias eliminam diatomáceas, por competição em nutrientes inorgânicos (azoto e fósforo), devido à grande concentração de carbono orgânico dissolvido. Contudo, num sistema onde ocorra ressurgência costeira, diatomáceas devem ser o principal contribuinte para a biomassa fitoplanctônica, devido à alta concentração de silicato (Thingstad, et.al. 2007), usado por diatomáceas na sintese de frústulas (Amin, et.al. 2012). A influência da turbulência na dinâmica competitiva entre diatomáceas e bactérias heterotrófica, sob condições ambientais variáveis, foi estudada para determinar se esse fator influencia significativamente a situação competitiva. A implicação da influência da turbulência sobre a dinâmica de competição é importante para a avaliação do destino do azoto e do fósforo presentes no ambiente marinho. Considerando um ambiente dominado por bactérias heterotróficas, estes nutrientes inorgânicos serão reciclados, enquanto num ambiente dominado por diatomáceas, devido a processos como “sloppy feeding” e o afundamento das células, grande parte da concentração de nutrientes é exportada para fora do sistema.

Amostras de água foram recolhidas a 1km ao sul da marina El Masnou, localizada na região da Catalunha, a 18 de outubro de 1999. Estas amostras foram utilizadas em oito séries de experiências sob forma de microcosmos controlados. Quatro microcosmos foram submetidos à turbulência gerada mecanicamente por grelha ($\varepsilon = 0.055 cm^2\ s^{-1}$), enquanto os outras

quatro microscosmos foram mantidos em condições estáticas. Dos microcosmos turbulentos e não turbulentos, as quatro configurações ambientais variadas consistiam em glucose, utilizada para substituir o carbono orgânico dissolvido, glucose e silicato, silicato e um controle sem silicato nem glucose. Cada microcosmo recebeu inputs diários de azoto e fósforo. Os que continham silicato tiveram enriquecimento a cada dois dias, enquanto os com glucose tiveram uma única aplicação no dia 0. A duração da experiência foi de oito dias. Os níveis de silicato, fósforo, nitrato, nitrito e amônio foram medidos a cada dois dias. Amostras foram retiradas diariamente de cada microcosmo para análise de carbono orgânico dissolvido, clorofila a rácio biomassa autotrófica vs biomassa osmotrófica total e biomassa bacteriana.

A análise dos dados mostrou que, ao contrário da hipótese original, a turbulência não teve influência significativa no resultado da competição entre diatomáceas e bactérias heterotróficas. Especulou se que nos microcosmos havia sempre nutrientes suficientes disponíveis para o fitoplâncton, independentemente da turbulência, que geralmente favorece as diatomáceas aumentando o cisalhamento turbulento. Por esse processo de cisalhamento é passada, a maior parte dos nutrientes (Bergvist, et.al. 2018) auplementando a difusão pela membrana celular. Os microrganismos autotróficos beneficiaram da adição de silicato e foram capazes de superar as bactérias heterotróficas, independentemente da adição de glucose ou não. A biomassa bacteriana aumentou em ambos os microcosmos enriquecidos com glucose, porém foi observada um decréscimo acentuada no dia 4, que foi atribuído ao “grazing” por protozoários. Na presença de glucose e ausência de silicato, a biomassa autotrófica diminuiu rapidamente, exibindo um pico no

dia 4 antes de diminuir novamente. Aproximadamente no dia 8, voltou a aumentar, possivelmente devido ao “grazing” de heterotrófico ou mixotrófico sobre as bactérias heterotróficas resultando em remineralização substancial. A mesma situação foi observada na ausência de glucose e silicato, com um pico ocorrendo no dia 3. A atividade da clorofila *a* em ambos os microcosmos desprovidos de silicato foi consistentemente baixa, sugerindo uma taxa reduzida de produtividade primária das diatomáceas. Nos microcosmos contendo glucose, a produção primária aumentou por volta do dia 8, embora na ausência de glucose o aumento da produção tenha ocorrido mais lentmente e começou a diminuir após o dia 6. Isso coincidiu com uma diminuição da biomassa autotrófica no mesmo microcosmo. Esta diminuição também pareceu coincidir com um aumento na biomassa bacteriana, sugerindo remineralização dos autótrofos neste microcosmo. Houve uma diminuição previsível na biomassa autotrófica durante a ausência de glucose e silicato. Contudo essa biomassa pareceu aumentar rapidamente a partir do dia 5. Visto que a biomassa bacteriana permaneceu baixa neste microcosmo, especulou-se que o “grazing” eficaz por protozoáriosimpediu a produção mas promoveu remineralização, causando, assim, o aumento da biomassa exibida pelos autótrofos. Foi possível identificar diferenças na proporção de diatomáceas sobre dinoflagelados na presença ou ausência de turbulência. Essas diferenças eram esperadas, pois as diatomáceas possuem mobilidade reduzida em comparação aos dinoflagelados, que têm locomoção, enquanto as diatomáceas beneficiam da mistura turbulenta e da ressuspensão de nutrientes (Ross and Sharples, 2007). Com isso, é possível sugerir que, embora importantes, as diatomáceas não são o único componente

na competição fitoplanctônica envolvendo bactérias heterotróficas. Tal hipótese é apoiada pelo facto de que a turbulência não teve influência sobre essa competição, mas pareceu afetar a proporção de diatomáceas sobre dinoflagelados. Foi sugerido no presente estudo que a ausência de diatomáceas por falta de silicato permite que os dinoflagelados dominem a produção fitoplanctónica, tornando-se os principais competidores das bactérias heterotróficas.

O presente estudo identifica a desvantagem potencial na utilização de microcosmos para esse tipo de experiência. O volume relativamente pequeno pode impedir que os nutrientes minerais precipitem da solução. Porém este estudo mostrou que a dinâmica competitiva entre autótrofos e bactérias heterotróficas é altamente influenciada pelas concentrações ambientais de silicato e carbono orgânico dissolvido, e que o rácio de diatomáceas sobre bactérias heterotróficas é influenciado pela turbulência.

ACKNOWLEDGEMENTS

This study was supported by the Institut de Ciencias del Mar (CSIC) who provided the data and additional support and advice for the project and by the Universidade do Algarve who runs the Marine and Coastal Systems masters course. Thank you to Helena Galvão and Pedro Cermeño for their continuous support and assistance in writing this thesis. With their help the process was much more streamlined, and their comments helped create a body of work to a higher standard. Thank you to Elliot O'Neill and Jasmine Haskell for their assistance with data representation and advice on using RStudio. With their help, many of the figures in this thesis were created. Finally thank you to Tayna Nascimento for her continuous moral support throughout.

TABLE OF CONTENTS

DECLARAÇÃO DE AUTORIA DE TRABALHO / DECLARATION OF AUTHORSHIP OF WORK I

ABSTRACT **..... II**

RESUMO IV

ACKNOWLEDGEMENTS VIII

TABLE OF CONTENTS IX

LIST OF FIGURES XI

LIST OF TABLES XII

LIST OF ABBREVIATIONS XIV

1 INTRODUCTION 1

1.1 The role of heterotrophic bacteria in the microbial loop 2

1.2 The role of diatoms in the microbial loop 3

1.3 idealised minimum microbial loop 4

1.4 Effect of turbulence on diatom growth 5

1.5 Aims and objectives of the current study 5

2 METHODS 7

2.1 Study location 7

2.2 Experimental set-up 8

2.3 Variables measured 9

2.4 Nutrient and Chl *a* determination 9

2.5 DOC – Bacteria and autotrophic enumeration 10
2.6 Biomass calculations 11
2.7 Data analysis 12

3 RESULTS 15

3.1 Experimental data 15
3.2 Microcosms with glucose 20
3.3 Microcosms without glucose 22
3.4 Chlorophyll *a* 24
3.5 Bacteria 25
3.6 Autotrophic to total osmotrophic biomass ratio 27
3.7 Dissolved organic carbon 28
3.8 Behaviour of autotrophic to total osmotrophic biomass ratio 32
3.9 Trends in nutrients 34
3.10 Phytoplankton community composition 36

4 DISCUSSION 39

4.1 Influence of turbulence 39
4.2 Influence of Si 43
4.3 Competition between HB and Diatoms 46
4.4 Limitations of the study 49

5 CONCLUSION 51

REFERENCES 53

APPENDICES 61

LIST OF FIGURES

Figure 1 - Flow structure for mineral nutrients through the "minimum" model food web adapted from Thingstad, et.al. (2007). 4

Figure 2 – Image of sample location ca. 1km off the coast of El Masnou, Catalonia. Image taken using Google Earth Pro. 7

Figure 3 – Results for the microcosms with glucose, with and without turbulence for;- (a) Chl *a* with Si; (b) bacteria with Si; (c) autotrophic to total osmotrophic biomass (A/(A+HB)) ratio with Si; (d) DOC with Si; (e) Chl *a* without Si; (f) bacteria without Si; (g) A/(A+HB) without Si; (h) DOC without Si; from day 0 to day 8. .. 21

Figure 4 - Results for the microcosms without glucose, with and without turbulence for;- (a) Chl *a* with Si; (b) bacteria with Si; (c) autotrophic to total osmotrophic biomass ratio (A/(A+HB)) with Si; (d) DOC with Si; (e) Chl *a* without Si; (f) bacteria without Si; (g) A/(A+HB) without Si; (h) DOC without Si; from day 0 to day 8. .. 23

Figure 5 – Comparison of medians throughout the duration of the experiment with;- (a) Chl *a*; (b) bacteria; (c) autotrophs and (d) DOC..... 31

Figure 6 – Tendency of dominance for autotrophs (i.e. A/(A+HB) > 0.5) in;- (a) presence or absence of glucose; (b) presence or absence of Si; (c) presence or absence of turbulence. 32

Figure 7 – Temporal evolution;- (a) ammonium; (b) nitrate; (c) nitrite; (d) phosphate; (e) silicate for each of the mesocosm over 6 days of the experiment. 34

Figure 8 – Biomass ratio of diatoms to dinoflagellates under; (a) the treatments with Si: and (b) the treatments without Si. 36

LIST OF TABLES

Table 1 – Experimental set-up showing the concentrations of nitrogen (N), phosphorous (P), silicate (Si) and glucose (C) added to each of the 8 microcosms and the frequency of application. T indicates the presence or absence of turbulence in the microcosms. As explained in the main text, these experiments were performed using natural samples, which were filtered through 150µm nominal pore size nylon mesh to remove mesozooplankton. 9

Table 2 – Measurements of Chl *a* recorded for every day of the experiment for each of the 8 microcosms. C = organic carbon added in the form of glucose, CT = Glucose + Turbulence, CSi = Glucose + Silicate, CSiT = Glucose, Silicate + Turbulence, B = Control, BT = Turbulence, Si = Silicate and SiT = Silicate + Turbulence..... 15

Table 3 - Measurements of Bacterial cells recorded for every day of the experiment for each of the 8 microcosms. Notations are as in Table 2. 16

Table 4 - Measurements of autotrophic to total osmotrophic biomass ratios recorded for every day of the experiment for each of the 8 microcosms. Notations are as in Table 2. 16

Table 5 - Measurements of dissolved organic carbon (DOC) recorded for every day of the experiment for each of the 8 microcosms. Notations are as in Table 2. 17

TABLE 6 – Nitrate measured on day 0,2,4and 6 of the experiment. Notations are as in Table 2..... 17

Table 7 – Nitrite measured on day 0, 2, 4 and 6 of the experiment. Notations are as in Table 2..... 18

Table 8 - Ammonium measured on day 0, 2, 4 and 6 of the experiment. Notations are as in Table 2. 18

Table 9 - Phosphate measured on day 0, 2, 4 and 6 of the experiment. Notations are as in Table 2. 19

Table 10 - Silicate measured on day 0, 2, 4 and 6 of the experiment. Notations are as in Table 2. 19

LIST OF ABBREVIATIONS

- Alkaline phosphatase activity (APA)
- Ammonium (NH_4^+)
- Carbon and turbulence (CT)
- Carbon, silicate and turbulence (CSiT)
- Chlorophyll *a* (Chl *a*)
- Control (B)
- Dissolved organic carbon (DOC)
- Dissolved organic matter (DOM)
- Equivalent spherical diameter (ESD)
- Glucose (C)
- Heterotrophic bacteria (HB)
- High nucleic activity (HNA)
- Nitrate (NO_3^-)
- Nitrite (NO_2^-)
- Nitrogen (N)
- Phosphorus (P)
- Primary production/Net primary production (PP/NPP)
- Sedimentary diatom abundance (SDA)
- Silicate (Si)
- Silicate and turbulence (SiT)
- Total organic carbon (TOC)
- Turbulence only (BT)

1 INTRODUCTION

Despite being responsible for roughly 1% of global photosynthetic biomass, marine primary producers sustain half of global net primary production and almost five times their biomass of consumers (Bar-On, et.al. 2018). Understanding the structure and functioning of marine microbial communities is under scrupulous review and the knowledge gained in the field over the last three decades has highlighted the overwhelming importance of micro-organisms in controlling the ecological and biogeochemical functioning of ocean ecosystems (Cavicchioli, et.al. 2019). A growing awareness of the importance of heterotrophic bacteria (HB) and their influence on microbial food webs has been under rigorous review over the past 30 years (Azam, et.al. 1983; Thingstad, et.al. 2007). In coastal ecosystems, the key contributor to phytoplankton biomass are diatoms (Abrantes, et.al. 2016; Arin, et.al. 2002) which have complex and diverse ecological relationships with HB (Amin, et.al. 2012).

There are two main food webs in the marine environment. The microbial loop, which is typical of well-stratified, oligotrophic systems in which heterotrophic bacteria efficiently consume and remineralise most of the autotrophic biomass. On the contrary, in eutrophic systems such as coastal upwelling systems, diatoms dominate autotrophic primary production and most of their biomass is exported either to upper trophic levels, through the classical trophic chain or to the deep ocean and sediments, where it can be retained for time scales in the order of centuries to millions of years.

1.1 THE ROLE OF HETEROTROPHIC BACTERIA IN THE MICROBIAL LOOP

Heterotrophic bacteria are in direct competition with phytoplankton for mineral nutrients such as nitrogen (N) and phosphorus (P) which often limit the rates of primary production in oceanic surface waters (Chrzanowski, et.al. 1995; Kirchman, 1994; Sala, et.al. 2002). Under nutrient sufficient conditions typical of coastal upwelling systems, the growth of HB is limited by the availability of dissolved organic carbon (DOC). In this instance, diatoms become an invaluable source of DOC to the HB (Amin, et.al. 2012; Barbosa, et.al. 2001) particularly through the release of organic compounds exerting a strong influence on the activity and health of HB (Bratbak and Thingstad, 1985; Vargas, et.al. 2007).

In environments where the availability of DOC is in excess, HB become efficient competitors for mineral nutrients, limiting the growth of autotrophic organisms such as diatoms. Thus, high levels of DOC allow HB to outcompete diatoms and other phytoplankton for mineral nutrients (Diner, et.al. 2016). The competition between autotrophic organisms and HB has important implications on the carbon flux through marine ecosystems as the activity of HB increases the concentration of CO_2 in the surface waters whilst autotrophs detract from it through assimilation for photosynthetic processes (Diner, et.al. 2016). The superior competitive ability of HB for mineral nutrients (Guerrini, et.al. 1998; Amin, et.al. 2012) when DOC is in excess has a negative impact on diatom populations which are not able to satisfy their nutritional requirements (Drakare, 2002). Through advanced chemotaxis, HB have the added advantage over diatoms in that they are mobile and can “swim” towards inorganic and organic nutrient food sources (Amin, et.al. 2012).

1.2 THE ROLE OF DIATOMS IN THE MICROBIAL LOOP

Following periods of spring stratification, the first autotrophic planktonic organisms to bloom are diatoms (Allen, et.al. 2005). This is due to their high maximum nutrient uptake and large vacuole size for efficient nutrient storage capacity, leading to a rapid growth response to the initial addition of nutrients (Amin, et.al. 2012). Diatom growth and reproduction is limited mainly by the availability of dissolved silicate (Si) and other mineral nutrients, in particular N and P (NP). The latter two are resources for which they are in direct competition with HB. Diatoms have the ability to enter periods of dormancy following nutrient exhaustion during which they sink out of suspension because of their heavy silica frustules they form as a protective layer around the cells, often in the form of resting cysts, or through particle aggregation. This sinking of cell remains causes particulate organic carbon produced by the diatoms to be removed from the surface waters and sequestrated in deeper layers (Amin, et.al. 2012: Bergvist, et.al. 2018; Rynearson, et.al. 2013). This is particularly common in chain forming diatoms which make up the majority of diatom biomass in turbulent environments (Bergvist, et.al. 2018).

Under Si replete conditions, which take place in turbulent, upwelling systems and regions with high fluvial discharge, diatom growth is increased. The rapid growth of diatoms decreases the biomass of other phytoplankton such as dinoflagellates, coccolithophores or picophytoplankton through direct competition for nutrients but also possibly through the release of allelopathic chemicals. This highlights the role diatoms have in controlling the structure of phytoplankton communities (Dugdale and Wilkerson, 2001). It has been reported that under nutrient sufficient conditions, environmental Si concentrations >2µM trigger diatom blooms. This

causes an exhaustion of nutrients and a decrease or suppression of the growth rate of other phytoplanktonic species, which are unable to compete against diatoms (Egge and Aksnes, 1992; Havskum, et.al. 2003).

1.3 IDEALISED MINIMUM MICROBIAL LOOP

Thingstad, et.al. (2007) created a "minimal" model of a planktonic foodweb which shows the flow of inorganic and organic nutrients; Si, N, P and DOC through different biotic compartments. Figure 1 is a modified, simplified version of that model.

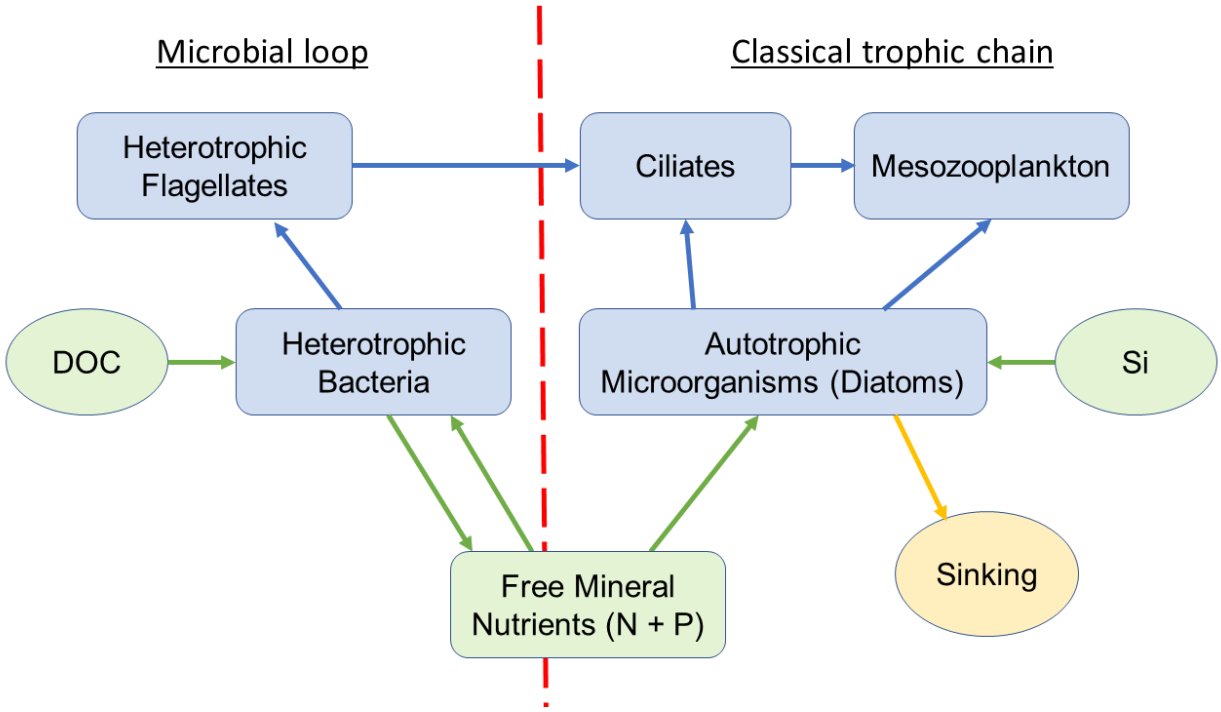

FIGURE 1 - Flow structure for mineral nutrients through the "minimum" model food web adapted from Thingstad, et.al. (2007).

The HB and diatoms are both in direct competition for the free mineral macronutrients, primarily nitrogen and phosphorus (NP). If DOC is in excess, the HB shall outcompete the diatoms for NP, facilitating the decomposition of organic matter and remineralisation of nutrients within the food web. Under sufficient Si concentrations

and lack of DOC, diatoms will outcompete the HB, stripping out NP from the system as diatoms sink out into the mesopelagic ocean.

1.4 Effect of turbulence on diatom growth

The food-web model (Figure 1) shows how the competition between diatoms and HB is affected by the presence or absence of both Si or DOC and its subsequent impact on the fate of the mineral nutrients in contrasting ocean environments (e.g. the well-stratified Mediterranean Sea versus a coastal upwelling system). However, it fails to account for the effect that turbulence has on diatom populations and therefore, on the entire respective food-web.

Turbulent shear is the increased movement across the cell caused by turbulence, and it enables a more rapid assimilation of carbon and other mineral nutrients by diatoms, particularly chain-forming species (Bergvist, et.al. 2018).

Turbulent mixing also impacts the time that photoautotrophic organisms experience favourable light conditions in the upper mixed layer. In stratified environments, organisms with superior buoyancy and/or autonomous motility will persist longer in the sunlit layers of marine and lacustrine environments. Diatoms, however, are better adapted to grow under fluctuating light conditions, characteristic of turbulent environments (Huisman, et.al. 2004).

1.5 Aims and objectives of the current study

This study aims to explore the competitive dynamics of HB and diatoms under laboratory-controlled conditions of nutrient supply and turbulence. This shall include the addition or privation of glucose, as a source of dissolved organic carbon (DOC) and the presence or absence of dissolved silicic acid (Si). This shall be carried out in

two different environments, one with no turbulence, simulating a stratified system, and another with synthetic turbulence in order to simulate unstable conditions typical of upwelling systems or environments with high submesoscale activity.

The work conducted herein shall provide insight as to the influence of nutrient supply dynamics and turbulence on the structure and functioning of marine microbial planktonic communities. This shall allow an improvement to current models used in this area of research informing ocean plankton ecosystem models encompassing contrasting hydrographic conditions. Chiefly, those that are permanently well stratified, and those that are subject to vertical mixing and turbulence.

From this, it shall be possible to gain a better understanding as to the impacts that a change in the marine environment will have on the microbial food webs, which, in turn, influence marine ecosystem services. This study shall add to the pool of work looking into the ecology of the marine microbiology and expand on what is known thus far. With a rise in atmospheric CO_2, global warming will increase ocean stratification, decreasing the input of inorganic nutrients to the surface. Thus, it is imperative to understand the response and ecological interactions of marine micro-organisms such as diatoms, which are responsible for roughly 20% of global net primary production and contribute disproportionately to the export of organic carbon into the deep ocean through the so called biological pump.

2 METHODS

2.1 STUDY LOCATION

The site of sample collection was ca. 1km off the coast from El Masnou, Catalonia in the Mediterranean Sea (Figure 2), which is characterised by a well stratified water column during summer and autumn.

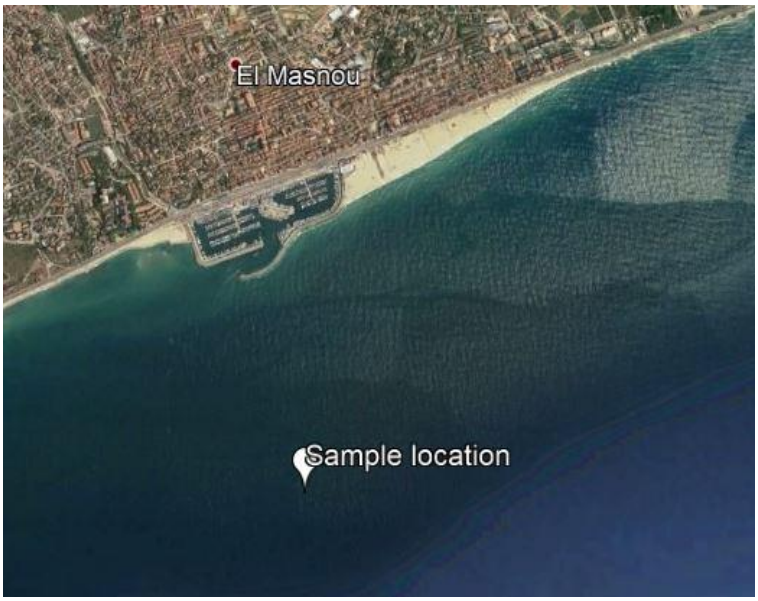

FIGURE 2 – Image of sample location ca. 1km off the coast of El Masnou, Catalonia. Image taken using Google Earth Pro.

The samples were analysed at Instituto de Ciencias del Mar in Barcelona, a research center belonging to the Spanish National Research Council (CSIC).

The microcosm experiments were run for 8 days each which is within the same time scale typical of an upwelling event (Wetz and Wheeler, 2004).

2.2 EXPERIMENTAL SET-UP

The samples were collected on the 18-10-1999 from surface waters 1km offshore from Masnou, Catalonia. Analysis of data was performed throughout the year 2020. Those who analysed the data to produce the current paper were not present during the collection and lab procedures, however, a constant liaison was maintained throughout.

Mesozooplankton organisms were discarded from the samples by washing them through a 150µm nylon mesh before the water was stored in sealed 15L cylindrical metacrylate containers with a height of 34.5cm and an inner diameter of 24.2cm.

A laboratory-controlled walking chamber was used to run the incubation experiments. The samples were subject to a 12:12, light:dark photoperiod with a saturating light irradiance of ~225µmol photons $m^{-2}s^{-1}$.

A grid generated turbulence (ε = 0.055cm^2 s^{-3}) was applied to four of the microcosms using the system described by Peters, et.al. (2002). The remaining microcosms were maintained under still conditions throughout the duration of the experiment.

Groups of containers were set-up with enrichments of either glucose, Si, glucose and Si and a control with neither glucose nor Si (Table 1). Two replicates of each enrichment variate were set-up. N and P were added daily to all containers at Redfield ratios (16:1, N:P). By adding nutrients in this way, biodegradable organic matter is available with a constant replenishment of low doses of mineral nutrients entering the system in what would be through mixing or resuspension in nature.

TABLE 1 – Experimental set-up showing the concentrations of nitrogen (N), phosphorous (P), silicate (Si) and glucose (C) added to each of the 8 microcosms and the frequency of application. T indicates the presence or absence of turbulence in the microcosms. As explained in the main text, these experiments were performed using natural samples, which were filtered through 150µm nominal pore size nylon mesh to remove mesozooplankton.

Experimental design

	Nutrient concentrations in µM			
Nutrient	N	P	Si	Glucose
Initial	0.65	0.08	0.91	N/A
Addition NP/NPT	2	0.125		
Addition NPSi/NPSiT	2	0.125	4	
Addition NPC/NPCT	2	0.125		15.6
Addition NPSiC/NPSiCT	2	0.125	4	15.6
Frequency	Daily	Daily	Daily	Once

2.3 VARIABLES MEASURED

The experiment was carried out over an 8-day period and all the parameters were monitored during this time Chl *a* (Table 2), heterotrophic bacteria (Table 3), autotrophs (Table 4) and DOC (Table 5) were measured daily. Mineral nutrients N and P were measured every second day and samples were taken from the microcosms on days 0, 4, 6 and 7 to analyse the taxonomic composition of phytoplankton communities. Estimations of the sedimented phytoplankton biomass were calculated by strongly mixing one replicate of each variant on day 4.

2.4 NUTRIENT AND CHL *A* DETERMINATION

Nitrate (Table 6), nitrite (Table 7), ammonium (Table 8), phosphate (Table 9) and silicate (Table 10) concentrations were determined (figure 7) using an Alliance Evolution II autoanalyzer using minor

modifications to the methods set out by Grasshoff (1983). Chl *a* concentrations were estimated fluorometrically (Yentsch and Menzel, 1963). 20ml samples were filtered through Whatman GF/F filters. Chl *a* was extracted by grinding the samples in 90% acetone solution and leaving them in the dark at room temperature for at least 2 hours. A Turner Designs fluorometer was used.

2.5 DOC – BACTERIA AND AUTOTROPHIC ENUMERATION

The abundance of bacteria was determined using flow cytometry (Gasol and del Giorgio, 2000). 1.2ml samples were fixed using 1% paraformaldehyde + 0.05% glutaraldehyde. Thereafter, they were left in the dark at room temperature for 10 minutes before storage at 70°C. The samples were then thawed for use at a later date. They were run through a Becton and Dickson FACScalibur flow cytometer with a laser emission at 488nm.

A subsample of 200µl was extracted and stained with Syto13 (Molecular Probes) at 1.6µM (diluted in DMS) and left for 15 minutes to stain in the dark allowing bacterial abundance to be determined. The subsamples were run at ca. 12µl min^{-1} and the data was plotted logarithmically until 10,000 events had been processed. As an internal standard, 10µl of a 10^6 ml^{-1} solution of yellow-green 0.92µm Polyscience latex beads were added. The bacteria were detected using the specific signature in a plot of side scatter (SSC) vs. FL1 (green fluorescence).

Samples of autotrophic nanoflagellates were fixed using 10% glutaraldehyde (final conc. 1%). 20ml were then filtered through 0.8µm black polycarbonate filters and stained with DAPI (5µgl^{-1} final conc.). The filters were stored at -20°C. A Nikon Labphot epifluorescence microscope was used at 1250x magnification (Porter

and Feig, 1980) to count the autotrophic nanoflagalletes. The organism sizes were determined using a calibrated ocular micrometre in 3 size classes; 4-8µm, 8-16µm and >16µm.

For the identification and enumeration of the rest of the phytoplankton cells (chiefly diatoms, dinoflagellates and coccolithophores), samples were fixed with formolhexamine solution (0.4% final conc.). Counts were made using the technique set out by Utermöhl (1958) using 50cm^3 settling chambers. One of the chamber transects was observed at 400x magnification to count the smaller (<20µm of equivalent spherical diameter, ESD) and more frequent organisms and another transect or half of the chamber was observed at 200x magnification to count cells of intermediate cell size generally between 20 and 50µm of ESD. The whole chamber was scanned at 200x magnification count the largest organisms. All observed organisms were classified to the lowest possible taxonomic level.

2.6 Biomass calculations

Estimations of bacterial biomass were made by flow cytometry following the methodology set out by Gasol and del Giorgio (2000) using a biovolume to carbon conversion factor of 0.35µgC µm^{-3} (Bjørnsen, 1986). The values for autotrophic carbon biomass were calculated using a carbon to Chl *a* conversion factor of 30µgC per µg Chl *a*.

Volumes of *Synechoccus* sp. and picoeukaryotes given in Ribes et.al. (1999) from samples taken in March from the Northwest Mediterranean sea were used to calculate the biovolumes of these organisms. For *Synechoccus* sp., a mean carbon content value derived from Bjørnsen, (1986), Kana and Gilbert (1987) and Verity

et.al. (1992) was used (0.357pgC μm^3). For picoeukaryotes the biovolume to carbon conversion factor proposed by Verity, et.al. (1992) (pgC $cell^{-1}$ = 0.433 x $(\mu m^3)^{0.863}$) was accepted.

The cell volumes of autotrophic nanoflagellates (>4µm) was calculated from the mean size of each size class assuming an ellipsoidal cell shape. The biovolume to carbon conversion factor used in this case was the same as that used for the picoeukaryotes.

Biomass estimations for the diatoms, dinoflagellates and coccolithophores were similarly obtained from size measurements. A minimum of 20 individuals of the most abundant forms were recorded with a Hitachi KPC503 video camera at 400x magnification. Thereafter, the length and width of each organism was measured using NHImage software and the cell volumes calculated using a geometrical approximation of the shape of the cell. The carbon content was estimated from the biovolume to carbon conversion factor described in Montagnes et.al. (1994) (pgC $cell^{-1}$ = 0.109 x $(\mu m^3)^{0.991}$).

2.7 Data analysis

All data analysis was performed using RStudio version 3.5.3. The entire data set was subject to a Shapiro-Wilk test for normality (appendix I) and determine to be mainly not normally distributed due, in part, to the small sample size and random distribution clearly determinable by the Q-Q plots and histograms (Appendix VII, VIII, IX and X). Therefore, a Kruskal Wallis chi squared test was used to analyse the variance between groups (Appendix III, IV, V and VI). A post-hoc Dunn test was performed to determine where the significant differences between groups were. Due to the large number of groups, a Bonferroni adjusted alpha (0.05/28) was applied to the

results of the Dunn test to increase the confidence in the output (Appendix III, IV, V and VI). A Wilcoxon rank sum test was used to determine the influence of Si and turbulence on the ratio of diatoms to dinoflagellates. The standard deviation, variance and mean of the data set was also computed (Appendix II).

3 RESULTS

The data plotted herein contains the experimental data collected on the 18-10-1999, with all the subsequent analysis performed throughout the year 2020.

3.1 EXPERIMENTAL DATA

TABLE 2 – Measurements of Chl *a* recorded for every day of the experiment for each of the 8 microcosms. C = organic carbon added in the form of glucose, CT = Glucose + Turbulence, CSi = Glucose + Silicate, CSiT = Glucose, Silicate + Turbulence, B = Control, BT = Turbulence, Si = Silicate and SiT = Silicate + Turbulence.

Chl *a* (µg/L)

	With glucose				Without glucose			
Time (days)	C	CT	CSi	CSiT	B	BT	Si	SiT
0	1.65	1.65	1.65	1.65	1.65	1.65	1.65	1.65
1	0.6788	1.131	0.9165	1.248	0.9945	1.17	0.936	1.014
2	1.092	1.599	1.768	2.08	1.404	1.768	1.924	1.638
3	1.092	1.664	1.3	1.976	1.17	1.924	3.9494	4.1962
4	1.222	1.82	1.456	1.976	0.936	1.404	4.6899	6.2532
5	0.7076	0.845	1.287	1.391	0.858	1.638	5.8829	7.8
6	0.936	0.6829	3.4968	2.962	1.95	3.538	8.32	10.92
7	1.872	1.768	8.84	12.87	3.4968	4.443	7.1582	10.4
8	2.418	3.8259	6.788	39.494	5.1835	1.365	3.51	16.77

TABLE 3 - Measurements of Bacterial cells recorded for every day of the experiment for each of the 8 microcosms. Notations are as in Table 2.

Bacteria (cells/ml) ($x10^{-6}$)

	With Glucose				Without Glucose			
Time (days)	C	CT	CSi	CSiT	B	BT	Si	SiT
0	0.5	0.5	0.5	0.5	0.5	0.5	0.5	0.5
1	2.0	3.8	2.0	3.8	1.7	1.8	1.1	1.7
2	4.9	6.0	5.1	5.7	1.2	1.8	1.2	2.3
3	4.6	5.4	2.1	5.3	1.3	1.5	1.3	1.7
4	1.1	2.2	1.6	1.4	1.1	1.8	1.2	1.9
5	1.5	2.8	1.8		2.9	3.1	3.1	5.3
6	2.3	2.6	3.4		1.9	2.6	3.6	4.2
7	3.3	4.2	3.8		3.1	2.3	4.3	8.1
8	3.3	3.7	4.0		3.2	0.6	5.0	12

TABLE 4 - Measurements of autotrophic to total osmotrophic biomass ratios recorded for every day of the experiment for each of the 8 microcosms. Notations are as in Table 2.

Autotroph to total osmotrophic biomass (A/(A + HB))

	With glucose				Without glucose			
Time (days)	C	CT	CSi	CSiT	B	BT	Si	SiT
0	0.8068	0.8068	0.8068	0.8068	0.8068	0.8068	0.8068	0.8068
1	0.3058	0.2861	0.3575	0.3933	0.4455	0.4622	0.5258	0.4307
2	0.2195	0.261	0.3064	0.1855	0.6099	0.5682	0.6688	0.4931
3	0.2312	0.2808	0.4304	0.2763	0.5514	0.6192	0.7937	0.7541
4	0.5868	0.524	0.5321	0.5705	0.5227	0.4839	0.828	0.797
5	0.3707	0.272	0.472	0.4087	0.2833	0.3973	0.6951	0.6945
6	0.3259	0.2444	0.5582	0.5143	0.5623	0.6141	0.7362	0.7576
7	0.4169	0.3507	0.7404	0.7848	0.5847	0.7173	0.6757	0.6162
8	0.4855	0.566	0.683	0.8584	0.6663	0.7267	0.4629	0.6286

TABLE 5 - Measurements of dissolved organic carbon (DOC) recorded for every day of the experiment for each of the 8 microcosms. Notations are as in Table 2.

Dissolved organic carbon

	With glucose				Without glucose			
Time (days)	C	CT	CSi	CSiT	B	BT	Si	SiT
0	2.453	2.453	2.453	2.453	1.34	1.34	1.34	1.34
1	2.205	2.35	2.185	2.32	1.23	1.32	1.225	1.385
2	1.41	1.605	1.46	1.58	1.2	1.405	1.2	1.18
3	1.297	1.4927	1.1918	1.3607	1.32	1.1913	1.1715	1.1943
4	1.148	1.3755	1.1405	1.503	1.086	1.386	1.1765	1.2395
5	1.383	1.8058		1.596	1.003		1.113	1.077
6	1.432	1.616	1.491			1.129	1.343	1.516
7		1.913		1.538				1.332
8	1.31	1.57		1.6	1.32	1.64	1.262	1.65

TABLE 6 – Nitrate measured on day 0,2,4and 6 of the experiment. Notations are as in Table 2.

Nitrate

	With glucose				Without glucose			
Time (days)	C	CT	CSi	CSiT	B	BT	Si	SiT
0	0.24	0.24	0.24	0.24	0.24	0.24	0.24	0.24
2	0.16	1.58	0.11	0.90	3.63	4.07	3.46	2.92
4	1.76	2.71	1.15	3.26	6.38	4.16	1.23	4.27
6	5.59	6.50	3.54	6.70	8.06	10.00	0.46	0.14

TABLE 7 – Nitrite measured on day 0, 2, 4 and 6 of the experiment. Notations are as in Table 2.

Nitrite

	With glucose				Without glucose			
Time (days)	C	CT	CSi	CSiT	B	BT	Si	SiT
0	0.035	0.035	0.035	0.035	0.035	0.035	0.035	0.035
2	0.045	0.13	0.04	0.0925	0.1	0.1725	0.0475	0.11
4	0.0325	0.1825	0.0625	0.2775	0.0975	0.085	0.05	0.1425
6	0.125	0.32	0.055	0.395	0.11	0.125	0.06	0.05

TABLE 8 - Ammonium measured on day 0, 2, 4 and 6 of the experiment. Notations are as in Table 2.

Ammonium

	With glucose				Without glucose			
Time (days)	C	CT	CSi	CSiT	B	BT	Si	SiT
0	1.58	1.58	1.58	1.58	1.58	1.58	1.58	1.58
2	5.94	8.58	4.89	8.07	14.13	29.65	4.08	15.13
4	1.96	9.03	2.98	22.55	7.20	9.96	5.25	14.75
6	2.26	12.21	3.59	17.16	3.28	2.26	6.02	3.62

TABLE 9 - Phosphate measured on day 0, 2, 4 and 6 of the experiment. Notations are as in Table 2.

Phosphate

	With glucose				Without glucose			
Time (days)	C	CT	CSi	CSiT	B	BT	Si	SiT
0	0.07	0.07	0.07	0.07	0.07	0.07	0.07	0.07
2	0.10	0.10	0.06	0.08	0.25	0.30	0.21	0.21
4	0.33	0.23	0.27	0.37	0.49	0.27	0.25	0.21
6	0.34	0.30	0.33	0.32	0.50	0.34	0.27	0.21

TABLE 10 - Silicate measured on day 0, 2, 4 and 6 of the experiment. Notations are as in Table 2.

Silicate

	With glucose				Without glucose			
Time (days)	C	CT	CSi	CSiT	B	BT	Si	SiT
0	0.86	0.86	0.86	0.86	0.86	0.86	0.86	0.86
2	0.42	0.61	5.13	4.67	0.77	0.96	5.27	4.04
4	0.35	0.43	8.94	8.23	0.25	0.40	6.25	7.67
6	0.02	0.73	12.29	11.69	0.30	0.02	8.10	6.16

3.2 MICROCOSMS WITH GLUCOSE

All microcosms with glucose were plotted either with or without Si and comparing turbulent and non-turbulent environments in each panel of Figure 3.

With Si **Without Si**

(a) **(e)**

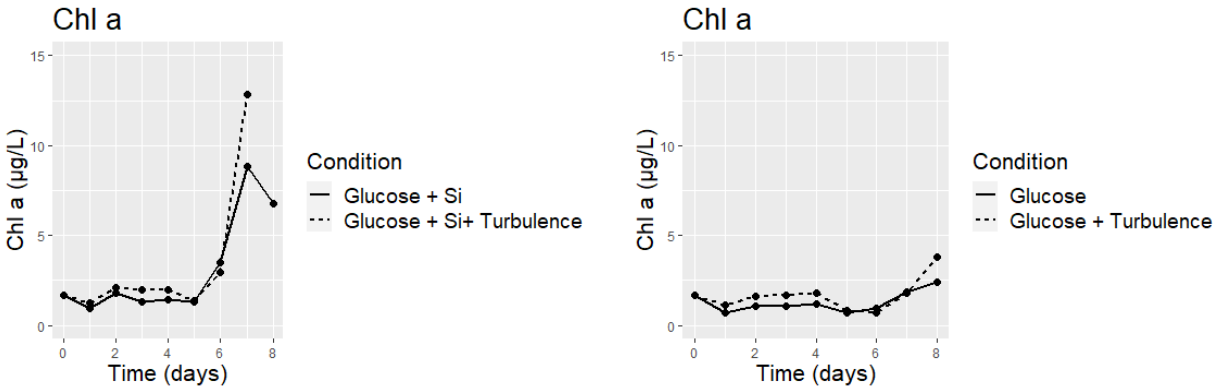

(b) **(f)**

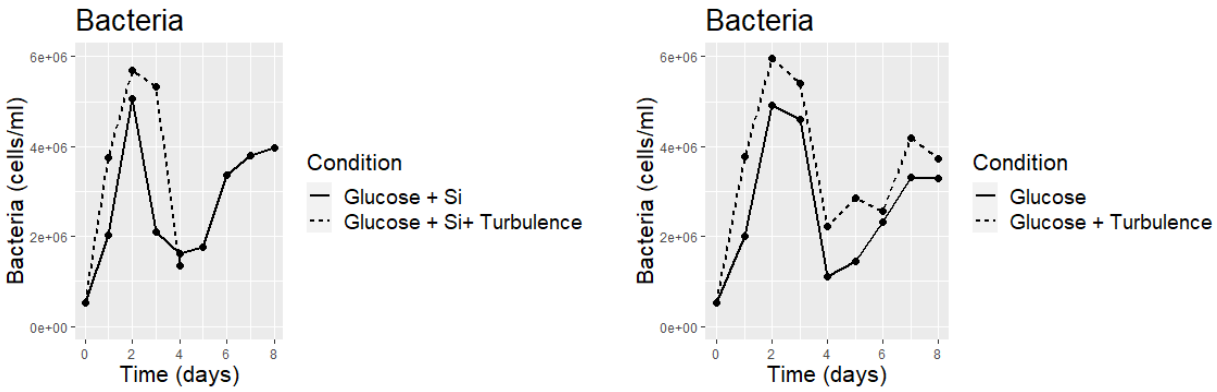

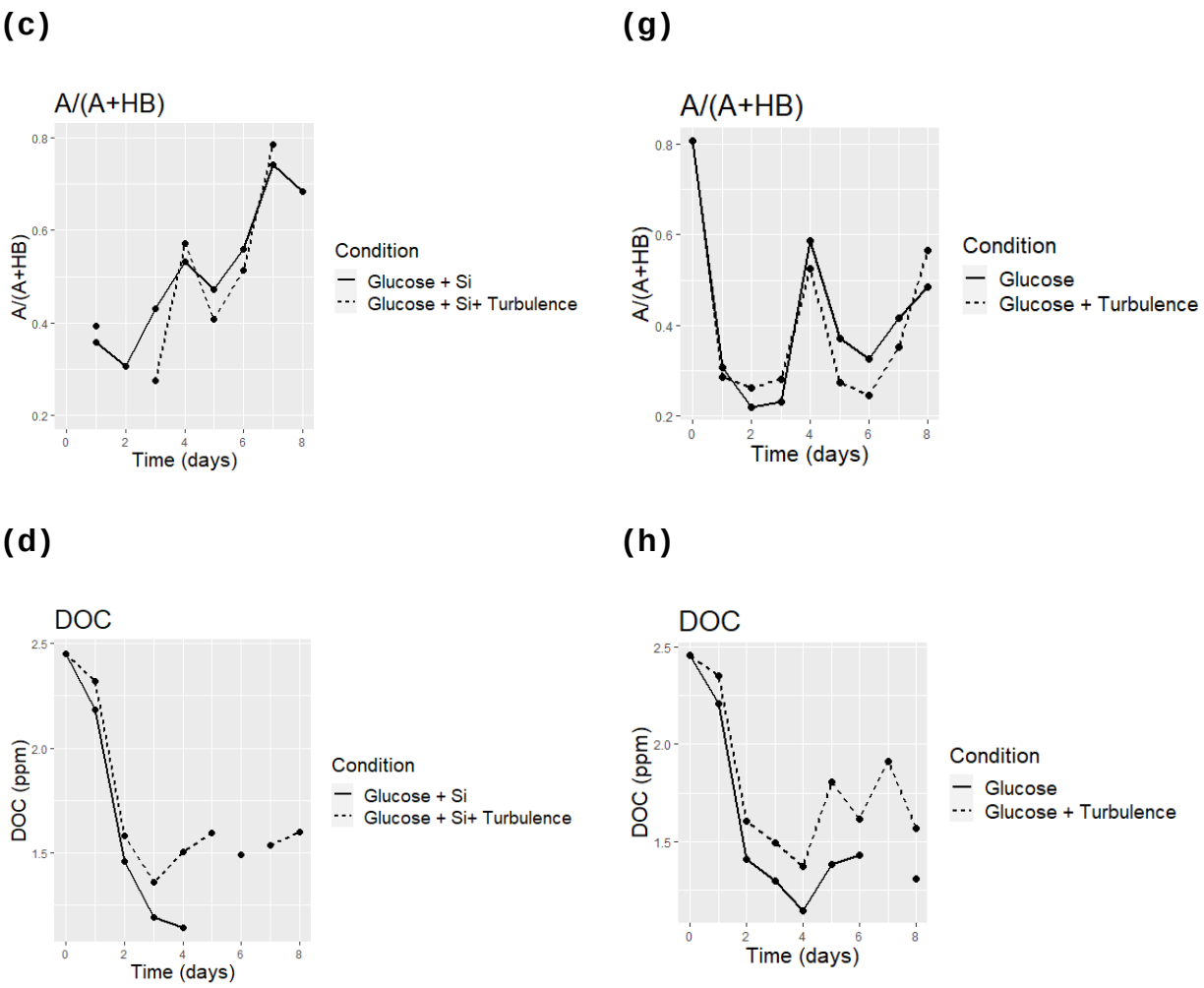

FIGURE 3 – Results for the microcosms with glucose, with and without turbulence for;- (a) Chl *a* with Si; (b) bacteria with Si; (c) autotrophic to total osmotrophic biomass (A/(A+HB)) ratio with Si; (d) DOC with Si; (e) Chl *a* without Si; (f) bacteria without Si; (g) A/(A+HB) without Si; (h) DOC without Si; from day 0 to day 8.

3.3 MICROCOSMS WITHOUT GLUCOSE

As in figure 3, the microcosms were plotted with and without Si and comparing turbulent and non-turbulent conditions but in this instance, only those without glucose supply were considered (Figure 4).

With Si **Without Si (control)**

(a) **(e)**

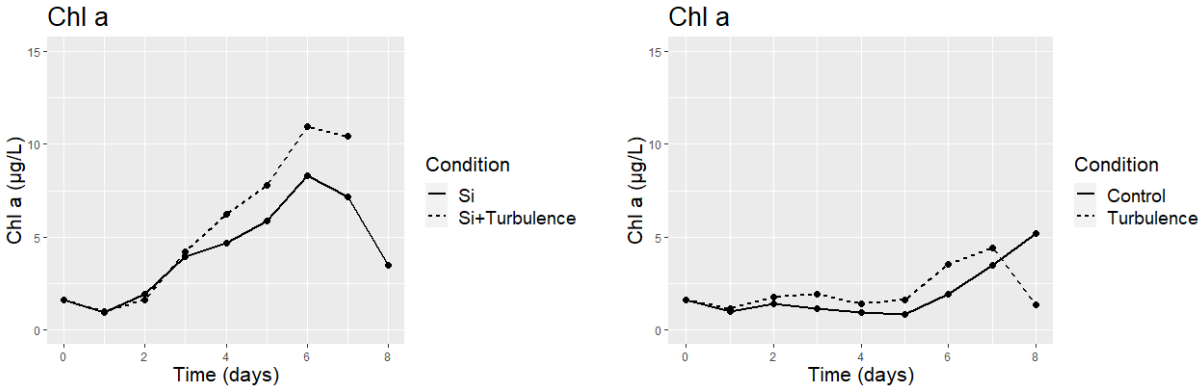

(b) **(f)**

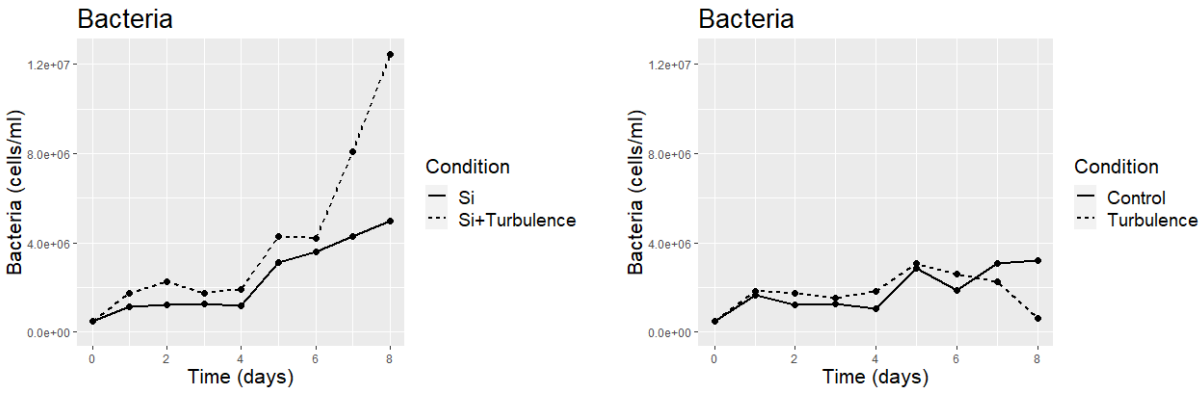

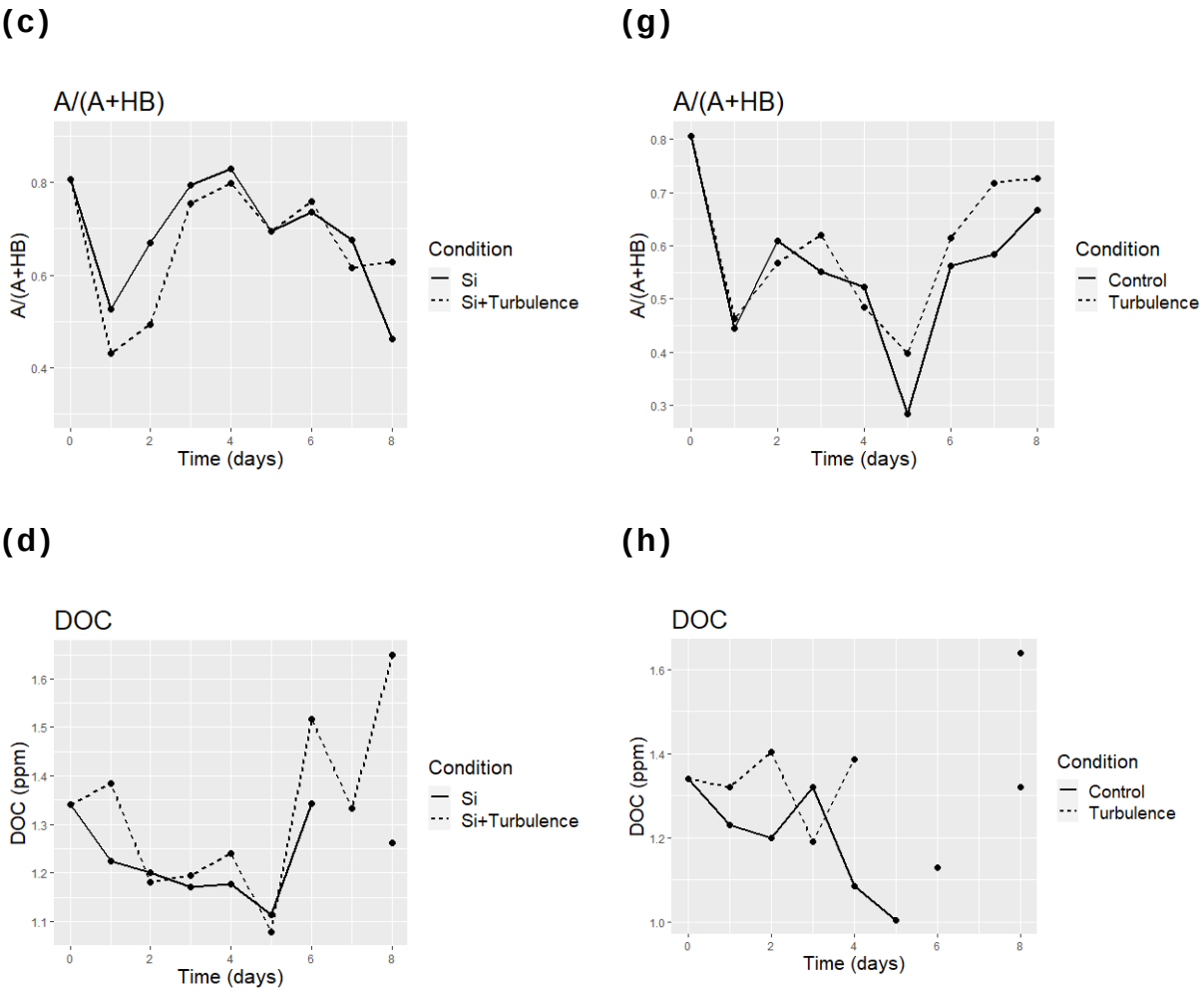

FIGURE 4 - Results for the microcosms without glucose, with and without turbulence for;- (a) Chl *a* with Si; (b) bacteria with Si; (c) autotrophic to total osmotrophic biomass ratio (A/(A+HB)) with Si; (d) DOC with Si; (e) Chl *a* without Si; (f) bacteria without Si; (g) A/(A+HB) without Si; (h) DOC without Si; from day 0 to day 8.

3.4 CHLOROPHYLL *A*

The results for Chl *a* were significantly different ($H(7) = 18.339$, $p = 0.01053$) between treatments. Following the Bonferroni test, the only significant difference between treatments for Chl *a* was between the Glucose treatment and the Si + Turbulence treatment ($z = -3.212$, $p = 0.037$) (Figure 5a). In the glucose treatment (Figure 3), both Si and Si + Turbulence treatments (Figure 3a) remained relatively constant below 2.5µg l^{-1} until day 5. Thereafter, the Si + Turbulence treatment incurred a rapid increase to 39.49µg l^{-1} by day 8 whereas the Si treatment increased to 8.84µg l^{-1} by day 7 before decreasing to 6.79µg l^{-1} by day 8.

In the glucose treatment without Si (Figure 3e), both treatments with and without turbulence incurred a decrease from day 0 to day 1. The treatment without turbulence saw a greater decrease in this time from 1.65 – 0.68µg l^{-1} compared to the .65 – 1.13µg l^{-1} decrease of the treatment with turbulence. Thereafter, both treatments saw a steady increase to day 4 with the non-turbulent treatment reaching 1.22µg l^{-1} and the turbulent treatment reaching 1.82µg l^{-1}. Following this, a rapid decrease in both treatments was observed. The non-turbulent treatment decreased to 0.71µg l^{-1} by day 5 before increasing to 2.42µg l^{-1} on day 8, whilst the turbulent treatment dropped to 0.68µg l^{-1} on day 6 before increasing to 3.83µg l^{-1} by day 8.

For treatments without glucose (Figure 4), there were some marked differences in Chl *a* concentration. For treatment with Si (Figure 4a), the Chl *a* concentration remained steady for the first two days, never increasing above 2.5µg l^{-1}. Thereafter, the treatment with turbulence increased to 16.77µg l^{-1} by day 8. The treatment without turbulence

increased to 8.32µg l^{-1} by day 6 before decreasing to 3.51µg l^{-1} by day 8.

For the treatment without glucose or Si (Figure 4e), the control dropped to 0.99µg l^{-1} on day 1, rose to 1.40µg l^{-1} on day 2 and then gradually decreased to 0.86µg l^{-1} on day 5. Following this, there was a rapid increase to 5.18µg l^{-1} on day 8. For the turbulent treatment, the concentration dropped to1.17µg l^{-1} on day 1 and then steadily increased to 1.92µg l^{-1} on day 3. Thereafter, it dropped once more to 1.40µg l^{-1} on day 4, rose steadily to 4.44µg l^{-1} on day 7 and then dropped rapidly to 1.37µg l^{-1} on day 8.

3.5 Bacteria

There was no statistically significant difference ($H(7) = 8.392$, $p = 0.2993$) in the heterotrophic bacteria cell count between any of the treatments used (Figure 5b).

In the glucose treatment (Figure 3), Si and Si + Turbulence (Figure 3b) displayed a rapid increase in the first two days, with the Si treatment reaching 5.08×10^6 cell x ml^{-1} and the Si + Turbulence treatment reaching 5.69×10^6 cells ml^{-1} by day 2. Thereafter, both treatments exhibited a rapid decrease in cell number until day 4 with the Si treatment dropping to 1.61×10^6 cells ml^{-1} and the Si + Turbulence treatment reaching 1.36×10^6 cells ml^{-1} due to grazing. Following this, the Si treatment increased again reaching 3.98×10^6 cells ml^{-1} by day 8. There was no further data available for the Si + Turbulence treatment.

For the treatment with glucose, without Si (Figure 3f), the trend is similar to Figure 3b described previously. In this case, there is a

rapid increase to day 2 with the turbulent treatment reaching $5.96x10^6$ cells ml^{-1} and the treatment without turbulence reaching $4.91x10^6$ cells ml^{-1}. Thereafter, they both exhibited a sharp decline with the turbulent treatment reaching $2.23x10^6$ cells ml^{-1} and the treatment without turbulence reaching $1.11x10^6$ cells ml^{-1} by day 8.

For the bacteria data without glucose and with Si (Figure 4b) the treatments with and without turbulence appeared to be similar for the first 6 days of the experiment. The turbulent treatment gradually increased, reaching $4.29x10^6$ cells ml^{-1} by day 5, dropping slightly to $4.22x10^6$ cells ml^{-1} on day 6 before increasing rapidly to $1.24x10^7$ cells ml^{-1} on day 8. The treatment without turbulence gradually increased to $4.99x10^6$ cells ml^{-1} on day 8 with a rapid increase between days 4 and 5 from $1.16x10^6$ to $3.14x10^6$ cells ml^{-1}.

In the data for treatments without Si or glucose (Figure 4f), the control condition increased from $5.13x10^5$ to $1.66x10^6$ cells ml^{-1} by day 1, before decreasing gradually to $1.06x10^6$ cells ml^{-1} on day 4. There was then a spike in the data on day 5 as it reached $2.87x10^6$ cells ml^{-1} before dropping to $1.86x10^6$ cells ml^{-1} on day 6. Following this, the cell-count rapidly increased to $3.20x10^6$ cells ml^{-1} by day 8. The treatment with turbulence incurred a similar increase by day 1 reaching $1.81x10^6$ cells ml^{-1}. Thereafter, there was a slight drop to $1.54x10^6$ cells ml^{-1} on day 3. Following this, the cell-count rapidly increased, reaching $3.08x10^6$ cells ml^{-1} on day 5, and finally dropping to $6.23x10^5$ cells ml^{-1} by day 8.

3.6 AUTOTROPHIC TO TOTAL OSMOTROPHIC BIOMASS RATIO

The results for the autotrophic to total osmotrophic biomass ratio (A/(A+HB)) were significantly different between treatments ($H(7) = 50.33$, $p = 1.244 \times 10^{-8}$). Following the Bonferroni test, the results from the Dunn test showed a significant difference between Control and Glucose + Turbulence ($z = 3.210$, $p = 0.037$), Glucose and Si ($z = -4.325$, $p = 0.0004$), Glucose + Si and Si + Turbulence ($z = -3.559$, $p = 0.010$), Glucose + Si + Turbulence and Si ($z = -3.706$, $p = 0.006$), Glucose + Turbulence and Si ($z = -4.506$, $p = 0.0002$), Glucose and Si + Turbulence ($z = 4.055$, $p = 0.001$), Glucose + Si and Si + Turbulence ($z = -3.514$, $p = 0.028$), Glucose + Si + Turbulence and Si + Turbulence ($z = -3.436$, $p = 0.017$), Glucose + Turbulence and Si + Turbulence ($z = -4.235$, $p = 0.0006$), Glucose and Turbulence ($z = -3.514$, $p = 0.012$) and Glucose + Turbulence and Turbulence ($z = -3.695$, $p = 0.006$) (Figure 5).

The A/(A+HB) results for the treatment with Glucose and Si (Figure 3c) shows an initial drop from 80.7% to 30.6% for the treatment without turbulence and 18.6% for the turbulent treatment on day 2. They both increased towards day 4 with the treatment without turbulence reaching 53.2% before dropping to 47.2% on day 5 and the turbulent treatment reaching 57.1% before dropping to 40.9% on day 5. Thereafter, the turbulent treatment reached 85.8% on day 8 whilst the treatment without turbulence reached 74.0% on day 7 before dropping to 68.3% on day 8.

For the treatment with glucose and without Si (Figure 3g), both the turbulent and non-turbulent treatments dropped rapidly from 80.7% towards day 2 with the former reaching 26.1% and the latter reaching 21.9%. Both treatments incurred a spike on day 4 with the non-turbulent treatment reaching 58.6% and the turbulent treatment

reaching 52.4%. They both dropped again by day 6 with the non-turbulent treatment falling to 32.5% before climbing once more to 48.6% on day 8 and the turbulent treatment falling to 24.4% before climbing to 56.6% by day 8.

For the treatments without glucose and with Si (Figure 4e), both treatments dropped rapidly by day 1 with the non-turbulent treatment dropping to 52.6% and the turbulent treatment dropping to 43.1%. By day 4 both had risen to 82.8% for the non-turbulent treatment and 79.7% for the turbulent treatment. Following this, both treatments dropped again with the non-turbulent treatment reaching 46.3% on day 8 and the turbulent treatment reaching 61.6% on day 7 and increasing slightly to 62.9% on day 8. There was a small increase between day 5 and 6 from 69.5% to 73.6% and from 69.5% to 75.8% for the non-turbulent and turbulent treatment, respectively.

3.7 Dissolved organic carbon

The results for DOC were significantly different between treatments ($H(7) = 27.948$, $p = 0.0002248$). Following the Bonferroni test the significant differences between treatments were between Control and Glucose + Si + Turbulence ($z = -3.360$, $p = 0.022$), Control and Glucose + Turbulence ($z = -3.696$, $p = 0.006$), Glucose + Si + Turbulence and Si ($z = 3.431$, $p = 0.017$) and between Glucose + Turbulence and Si ($z = 3.784$, $p = 0.004$) (Figure 5).

For the DOC treatments with Glucose and Si (Figure 3d), there was a rapid decline in both turbulent and non-turbulent treatments with the former dropping to 1.361g μl^{-1}. Before increasing steadily to 1.6g μl^{-1} by day 8 with data missing for day 6. Meanwhile, the non-turbulent treatment dropped to 1.141g μl^{-1} on day 4 before rising to 1.491g μl^{-1} on day 6. There was no data for days 5, 7 or 8.

For the treatments with glucose and without Si (Figure 3h), both treatments dropped rapidly by day 4 with the turbulent treatment falling to 1.376g μl^{-1} and the non-turbulent treatment falling to 1.148g μl^{-1}. Thereafter, the non-turbulent treatment steadily rose to 1.432g μl^{-1} on day 6 and then declined to 1.31g μl^{-1} on day 8 with data missing for day 7. The turbulent treatment fluctuated after day 4 reaching 1.806g μl^{-1} on day 5, 1.616g μl^{-1} on day 6, 1.913g μl^{-1} on day 7 and 1.57g μl^{-1} on day 8.

For the treatments with Si and no glucose (Figure 4d), the non-turbulent treatment dropped from 1.34g μl^{-1} to 1.113g μl^{-1} on day 5. It then rose to 1.343g μl^{-1} on day 6 before dropping to 1.262g μl^{-1} on day 8 with no data on day 7. Conversely, the turbulent treatment initially rose from 1.34g μl^{-1} to 1.385g μl^{-1} by day 1. It incurred a decline towards day 2 reaching 1.18g μl^{-1} then rose to 1.24g μl^{-1} on day 4. Thereafter, it fluctuated daily, reaching 1.077g μl^{-1} on day 5, 1.516g μl^{-1} on day 6, 1.332g μl^{-1} on day 7 and 1.65g μl^{-1} on day 8.

For the DOC treatments without glucose or Si (Figure 4h), the treatment without turbulence (control) dropped from 1.34g μl^{-1} to 1.2g μl^{-1} on day 2 before rising to 1.32g μl^{-1} on day 3 and then falling to 1.003g μl^{-1} on day 5. On day 8 the control was at 1.32g μl^{-1} with no data for day 6 or 7. For the turbulent treatment, there was daily fluctuation until day 4. The treatment dropped from 1.34g μl^{-1} to 1.32g μl^{-1} on day 1, then rose to 1.405g μl^{-1} on day 2, fell to 1.191g μl^{-1} on day 3 and rose to 1.386g μl^{-1} on day 4. Thereafter, by day 6 it had dropped to 1.129g μl^{-1} before rising to 1.64g μl^{-1} by day 8 with no data for days 5 or 7.

(a)

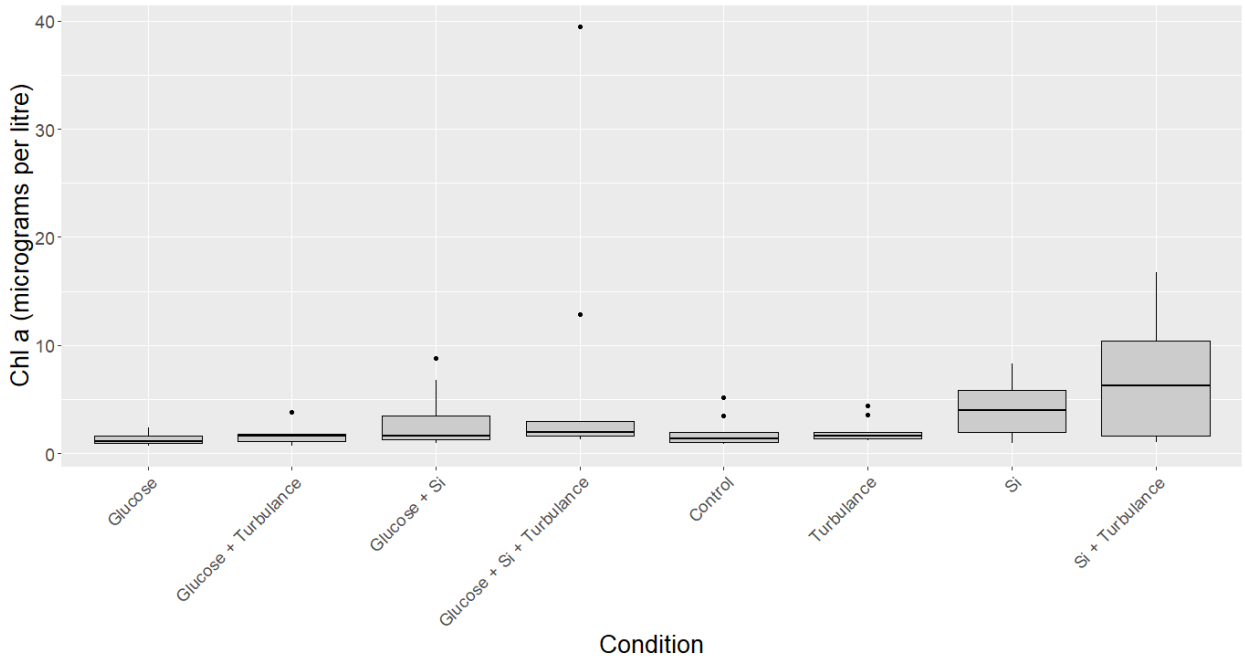
Chl a (micrograms per litre)
40
30
20
10
0
Glucose
Glucose + Turbulance
Glucose + Si
Glucose + Si + Turbulance
Control
Turbulance
Si
Si + Turbulance
Condition

(b)

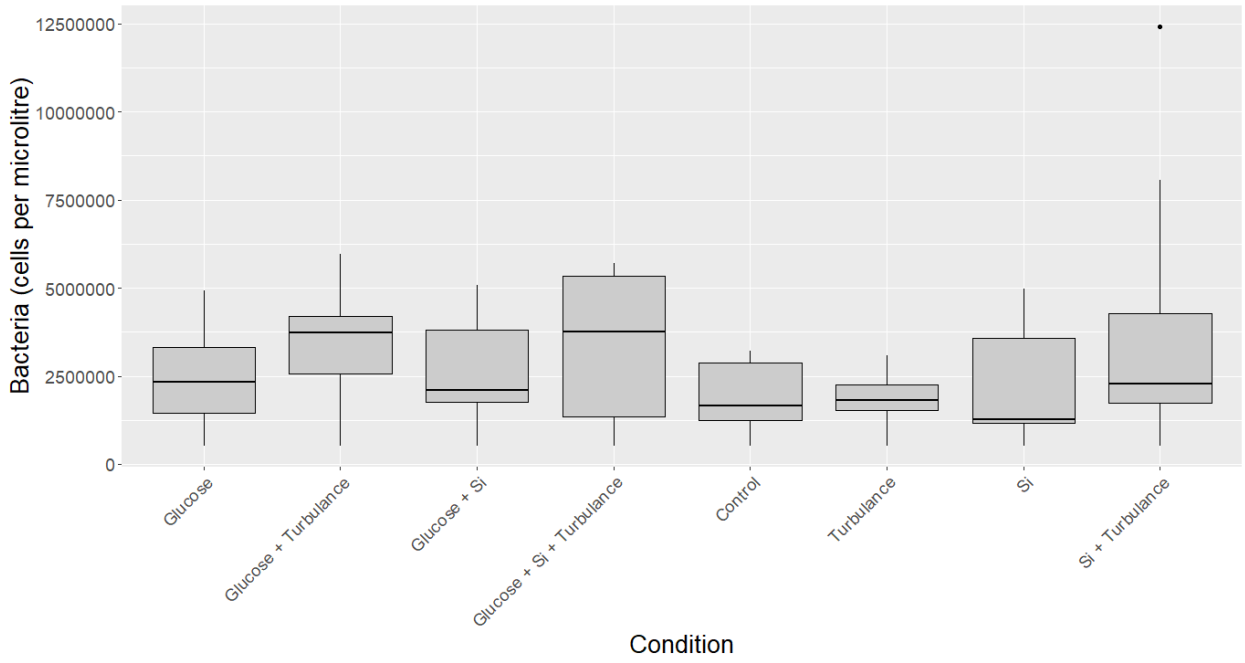
Bacteria (cells per microlitre)
12500000
10000000
7500000
5000000
2500000
0
Glucose
Glucose + Turbulance
Glucose + Si
Glucose + Si + Turbulance
Control
Turbulance
Si
Si + Turbulance
Condition

(c)

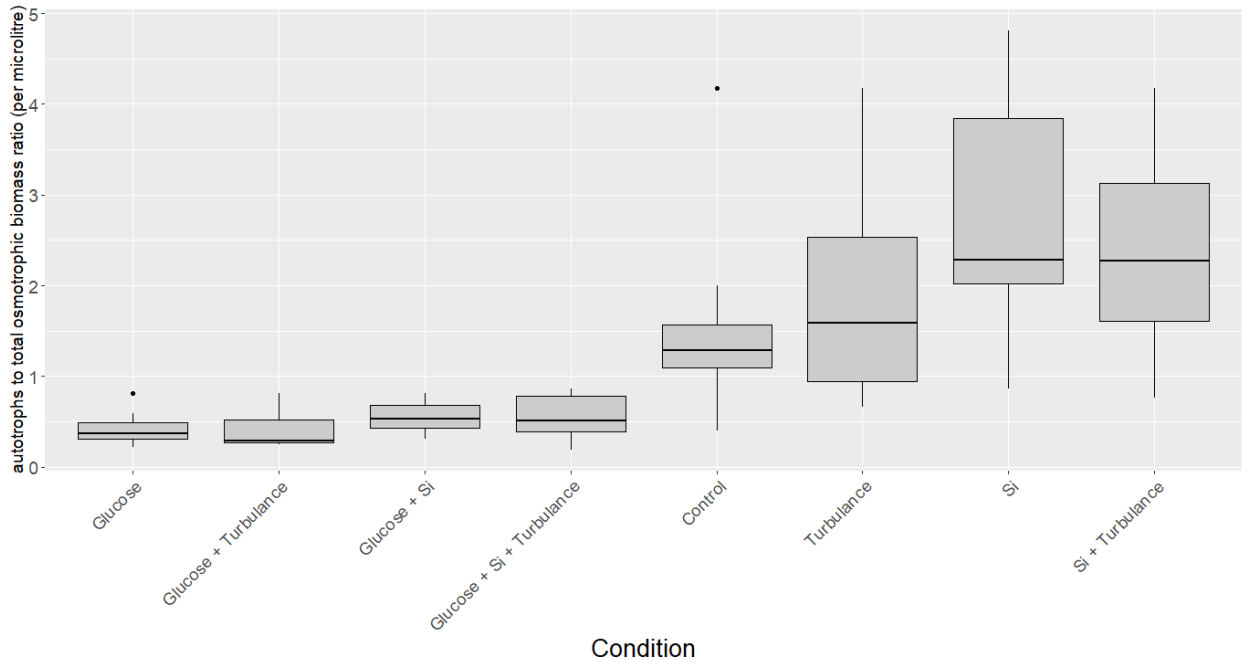

(d)

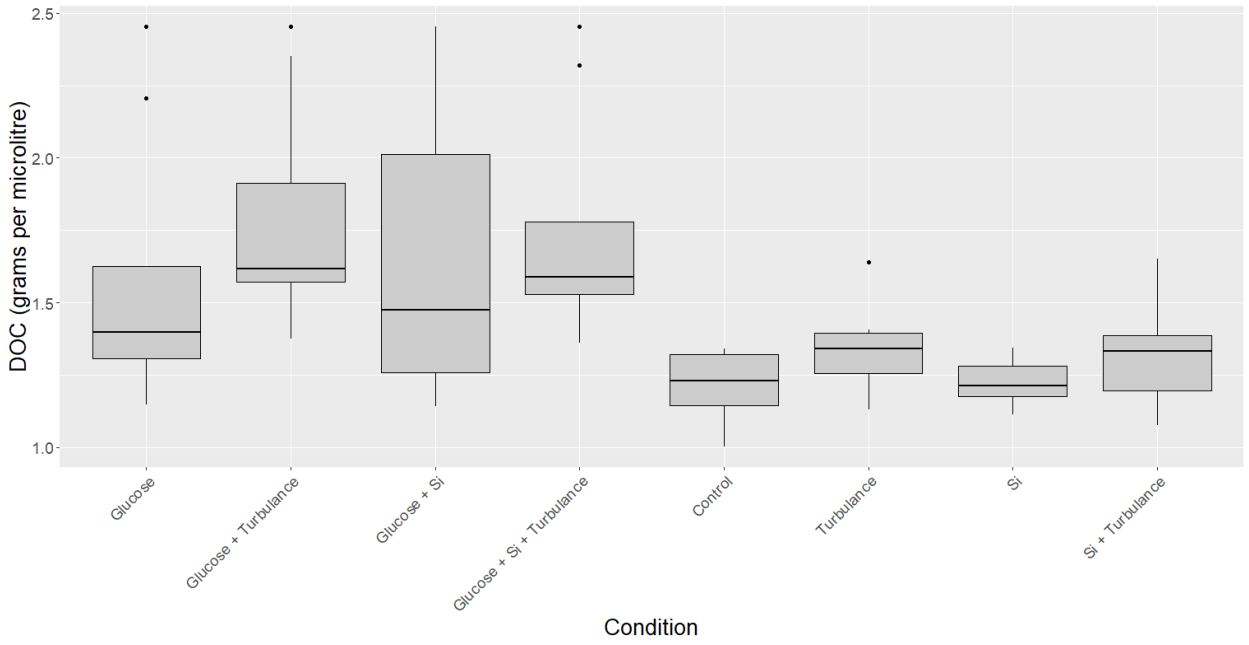

FIGURE 5 – Comparison of medians throughout the duration of the experiment with;- (a) Chl *a*; (b) bacteria; (c) autotrophs and (d) DOC.

3.8 BEHAVIOUR OF AUTOTROPHIC TO TOTAL OSMOTROPHIC BIOMASS RATIO

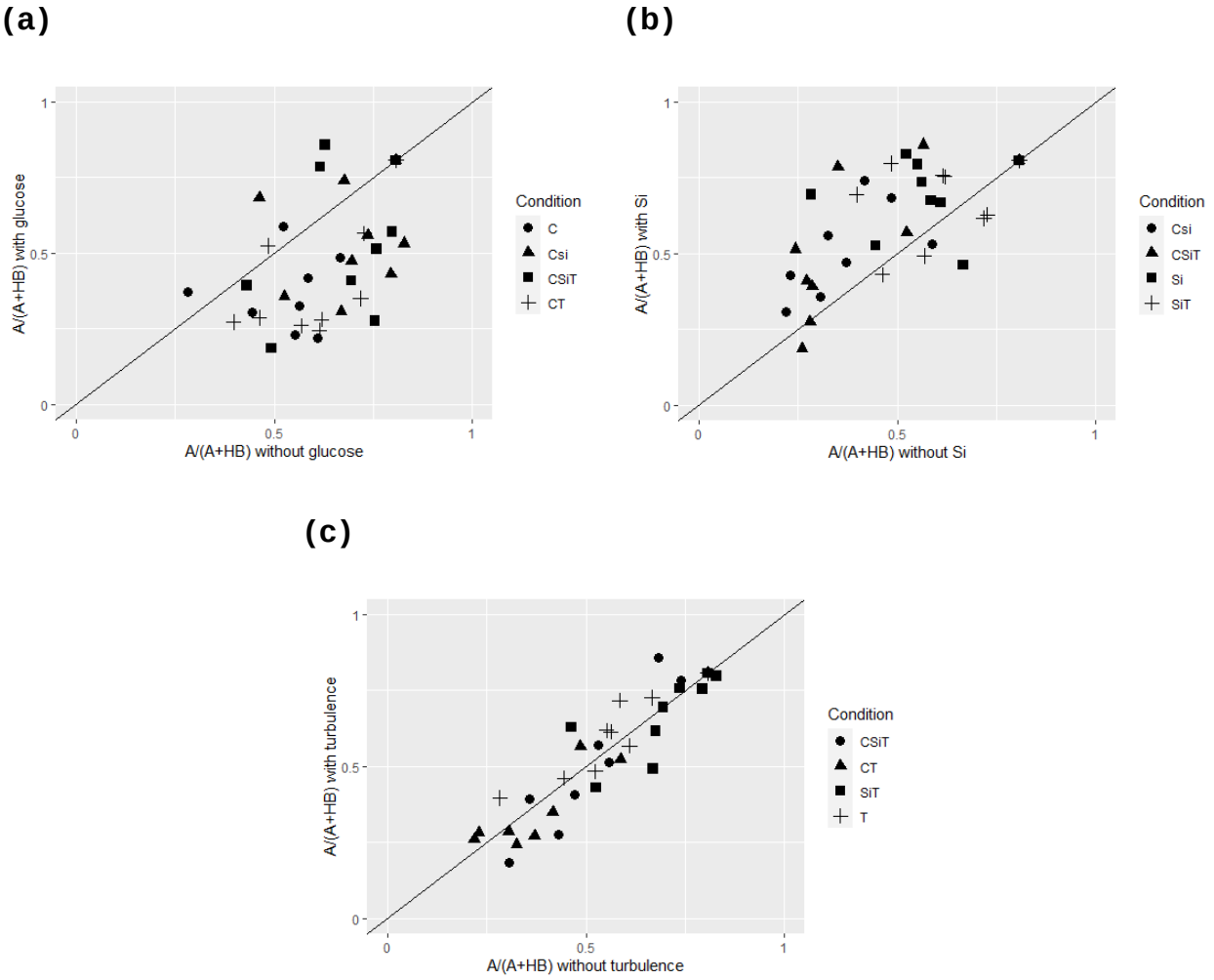

FIGURE 6 – Tendency of dominance for autotrophs (i.e. A/(A+HB) > 0.5) in;- (a) presence or absence of glucose; (b) presence or absence of Si; (c) presence or absence of turbulence.

With respect to autotrophs, a change in different physical parameters had varying results (Figure 6). When comparing treatments with and without glucose (Figure 6a) the majority of the data from the microcosms showed the autotrophs tended to favour the set-ups without glucose, as was to be expected. Likewise, as was the preconception, the autotrophs, primarily diatoms, were

favoured in the environments replete in Si (Figure 6b). Interestingly however, there seemed to be no real preference to an environment with or without turbulence (Figure 6c). The original hypothesis was that there would be a tendency for autotrophs (specifically diatoms) to favour a turbulent environment. This was not the case and will be discussed in detail.

3.9 TRENDS IN NUTRIENTS

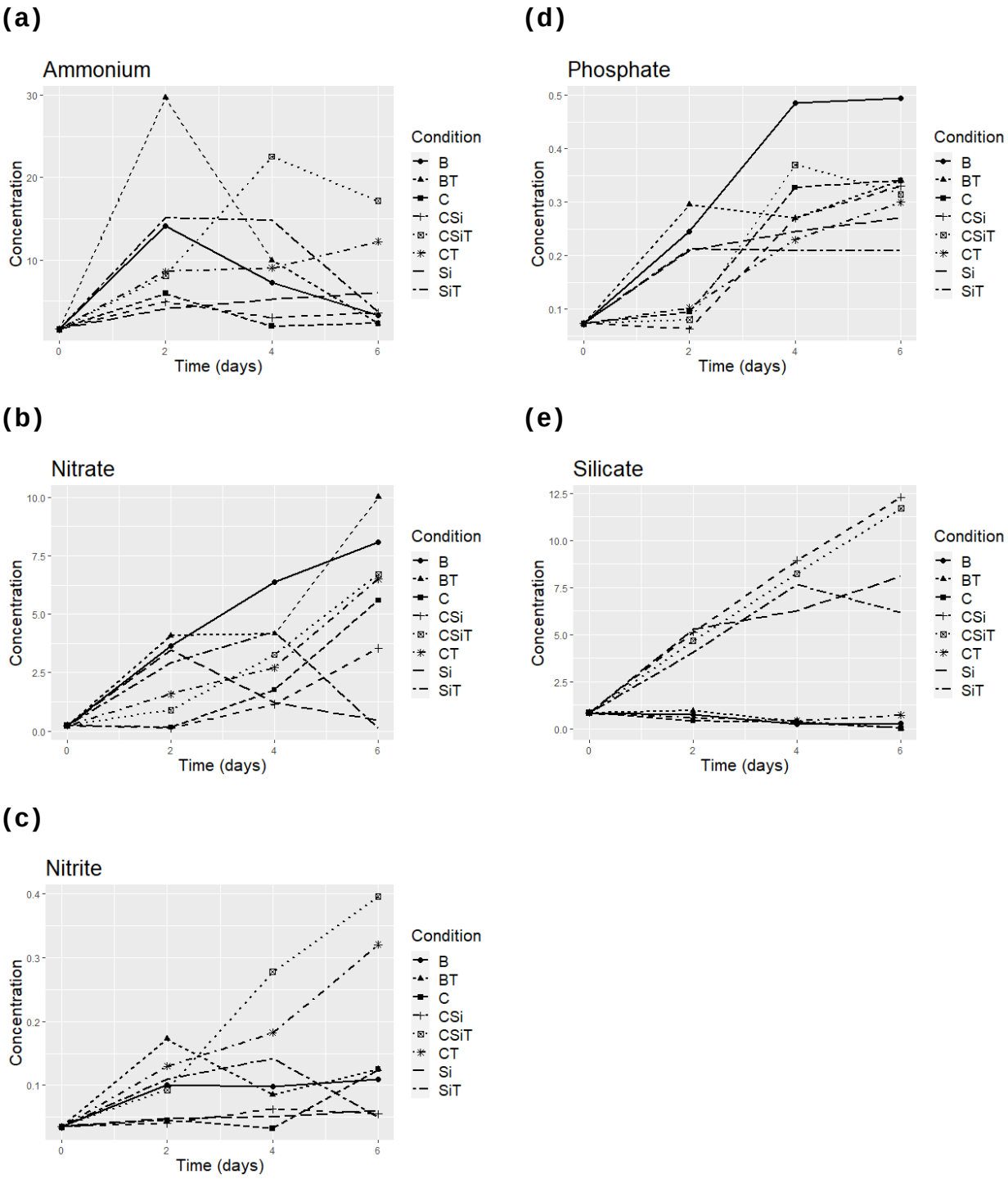

FIGURE 7 – Temporal evolution;- (a) ammonium; (b) nitrate; (c) nitrite; (d) phosphate; (e) silicate for each of the mesocosm over 6 days of the experiment.

Ammonium, nitrate, nitrite, phosphorus and silicate were recorded from day 0 to day 6 (Figure 7). Phosphorus was re-supplied to the microcosms daily and as was to be expected, increased throughout the experiment (Figure 7). Silicate (Figure 7e) only increased in the microcosms to which it was added. In those which were intended to have a deficiency, the recorded Si levels were consistently low. After day 4, the concentration of Si in the microcosm with Si and turbulence only, began to decrease towards day 6.

The ammonium (Figure 7a) in the C, CSi and Si treatments remained low throughout the 6 days of measurement. There was a gradual increase in the microcosm B and an increase and subsequent decrease in the BT and SiT microcosms. CT and CSiT on the otherhand, increased throughout the experiment.

The measurements of nitrate (Figure 7b) showed an increase in the CT, CSiT, CSi, C, B and BT microcosms, whilst the Si and SiT microcosms showed an initial increase in nitrate before decreasing towards day 6. The concentration of nitrite in the B and BT microcosms increased the most with a rapid increase in the BT nitrate concentration between day 4 and 6.

In the case of nitrite (figure 7c), only CSi and CSiT microcosms showed any real increase in the concentration of nitrite with CSiT recording the greatest concentration on day 6. Both SiT and BT saw an increase in nitrite to begin with before the concentration dropped again with a slight increase between day 4 and 6 for the BT microcosm reading. The remaining microcosms remained low in nitrite for the duration of the experiment. Nitrite concentration in the C microcosm did start to increase towards the end on the experiment but it is should not be assumed that this would continue to increase after day 6 as there is not enough data to back this up.

3.10 PHYTOPLANKTON COMMUNITY COMPOSITION

The biomass ratio of diatoms to dinoflagellates was plotted (Figure 8) to determine whether the various environmental parameters had any influence on phytoplankton community composition.

(a) **(b)**

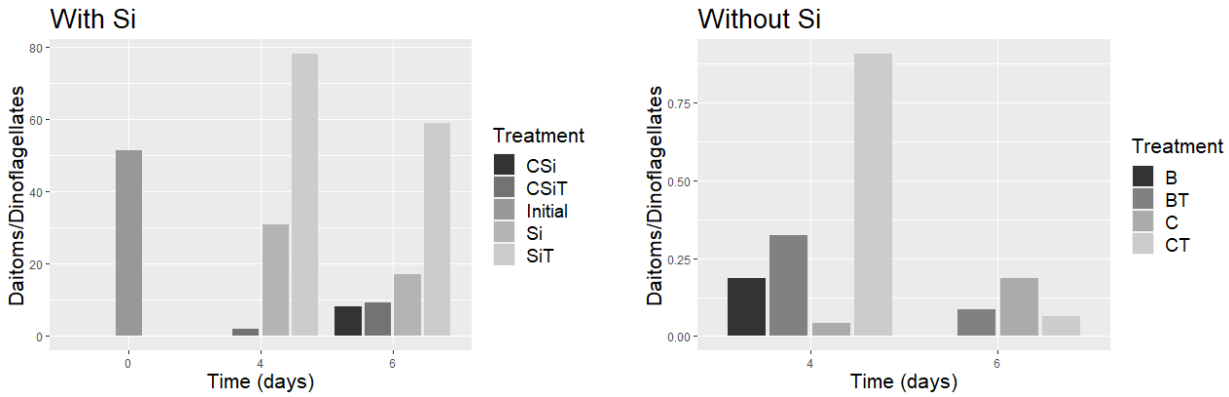

FIGURE 8 – Biomass ratio of diatoms to dinoflagellates under; (a) the treatments with Si: and (b) the treatments without Si.

There is an apparent difference in the ratio of diatoms to dinoflagellates (Figure 8) however, statistical analysis showed that this difference was not significant (W = 23, p = 0.3823). The difference between the glucose and silicate; and glucose silicate and turbulent treatments in the microcosms containing Si (Figure 8a) appears to be small, slightly favouring the turbulent treatment. The difference between the silicate; and silicate and turbulence treatments are noticeable whilst not significantly different on both day 4 and 6. In the microcosms without silicate (Figure 8b), the difference between the control and the turbulent control was very slight on day 4 and 6. The difference between the glucose; and the glucose and turbulent treatments was large but only on day 4. This was substantially smaller on day 6. The difference between the treatments with Si and without Si was significantly different (W = 60,

p = 0.001865) and shows a much greater ratio of diatoms to dinoflagellates in the presence of Si.

4 DISCUSSION

There have been many studies that aim to influence the structure and temporal dynamics of plankton communities under different environmental conditions. From a preliminary review of the literature, no investigation has yet been carried out on the influence of turbulence under different environments focussing on the presence or absence of DOC and Si. Contrary to the original hypothesis, the presence or absence of turbulence seldom made any difference to the competitive dynamics between phytoplankton and heterotrophic bacteria. However, the different availabilities of DOC and Si were found to influence the competitive dynamics between heterotrophic bacteria and diatoms, leading to a promotion of nutrient recycling through the microbial loop, or alternatively, nutrient losses through organic export.

4.1 INFLUENCE OF TURBULENCE

Because it is well understood that diatom abundance is often greater in upwelling systems (Abrantes, et.al. 2016; Arin, et.al. 2002), it was worth determining the influence of turbulence. Fatima, et.al. (2016) noted two important factors. Firstly, environments rich in Si will contain a high diatom abundance, and secondly, that turbulent upwelling systems relate to high levels of Si. In their study they used previous data from different global locations and found that diatom dissolution was mainly influenced by the concentration of Si saturation in the medium. Interestingly, they found that total organic carbon (TOC) was not related to sedimentation rate and neither was the sedimentary diatom abundance (SDA). They showed that, whilst it was true in some areas, oceanic physics did not appear to be a primary control on the magnitude of diatom blooms. They found there only to be a significant relationship in two southern

hemispheric systems: the Benguela and Humbolt upwelling systems. Furthermore, they found a positive relationship between SDA and net primary production (NPP), and between SDA and N and P levels. Again, the latter relationship was only true of certain areas and not a global trend. They found that in upwelling areas, there was a positive relationship between nitrate and SDA and silicic acid and SDA. This work is of interest because it suggests that the nutrients present in the system have more of an impact on both diatom abundance and diatom sedimentation, ergo carbon export, than upper ocean turbulence does. This may go some way to explain why in the current study, turbulence played no role in the phytoplankton community composition and the competitive dynamics between autotrophs and heterotrophic bacteria. Furthermore, the fact that the data collected by Fatima, et.al. (2016) was in situ data compared to the microcosm set up of the current study may also show a limitation in the methods used here. Most importantly, they showed that there is often a different outcome when the scope of sampling is local as compared to global sampling designs and trends seen in one area may differ to trends observed in other areas for various reasons. Turbulent mixing is still a seemingly important process as it controls both the availability of light and nutrients in a marine environment which determines the structure of the phytoplankton communities (Mouriño-Carballido, et.al. 2016). Furthermore, nitrate fluxes, not just its concentrations play an important role in oligotrophic environments (Mouriño-Carballido, et.al. 2016).

The effect of turbulence on diatom and bacterial competition under different N and P regimes was investigated in Arin, et.al. (2002), who found that turbulence often played a significant role in determining the phytoplankton community composition. They found that NP and Si decreased significantly faster in turbulent treatments

compared to still treatments in microcosms similar to those used in this study. In the current study, it was found that Si was slightly less in the SiT treatment than in the Si treatment. This was not a significant difference, however and there seemed to be an even smaller difference between CSi and CSiT treatments. Whilst this was not the subject of the current study, they also found a significant difference between N and NP treatments with and without turbulence. The results found here may back-up the fact that the concentrations of nitrogen and phosphorous are influenced by turbulence more-so than other nutrients and environmental factors when considering phytoplankton competition. They did not, however, find any significant difference in bacterial biomass in any of the containers between turbulent and still treatments. They found a higher ratio of diatoms to HB in the treatments with turbulence which suggests that diatoms are more affected by turbulent mixing than HB.

The perplexing fact that turbulence had no significant effect on any of the results of the current study could be explained upon reflexion of the paper by Gibson (2000). They studied the effects that different types of turbulence had on phytoplankton communities and what the effect of fossil turbulence, the resultant mixture of water following turbulent mixing, was. In their study they showed that diatoms are positively correlated to the intermittent, strong turbulence caused by the breaking of surface waves. Wind turbulence had little effect on the diatoms possibly because, when compared to wave turbulence, the effects were negligible. Their lab studies showed that diatoms responded negatively to fossil turbulence over time. The current study employed a constant mixing regime in the treatments with turbulence of ca. $0.55 cm^2\ s^{-1}$. Therefore, it is speculated here that a different outcome as to the

effect on turbulent mixing on community structures would have been obtained following a stagnated mixing approach.

In still waters, nutrient transport is largely associated with diffusive fluxes. Under turbulent condition, advective transport further facilitates nutrient supply and biological uptake and favours large cells (>ca. 60µm of equivalent spherical diameter) (Peters, et.al. 2006). This is one reason why diatoms are favoured over bacteria in turbulent environments. Peters, et.al. (2006) showed that larger species of diatoms, in this case *Cosconodiscus* sp. were favoured in turbulent conditions compared to the smaller species, *Thalassiosira pseudonana*. The important point to note here is that under P-limiting conditions, alkaline phosphatase activity (APA) increased to hasten P uptake, particularly under still conditions and only in the large-sized *Cosconodiscus* sp. This is important because it is mechanisms like this that allow diatoms to outcompete other planktonic organisms in nutrient limiting environments (Peters, et.al. 2006). It is speculated here that no such activity will have occurred in the current study due to the consistently high concentrations of NP. Therefore, a difference in competition between bacteria and diatoms would be more subtle. Not only was P never limiting in the current study, it was, in fact, constantly increasing in each microcosm throughout the experiment (Figure 7d).

The results from figure 8 showed that turbulence had an effect on the biomass ratios of diatoms to dinoflagellates, albeit not a significant difference. The ratio increased in most of the treatments that had been subjected to turbulence, thus favouring the diatoms. In natural coastal environments, following a diatom spring bloom, motile planktonic species such as dinoflagellates dominate the phytoplankton biomass when the water column stratifies (Ross and

Sharples, 2007). It is because of the motile capability of dinoflagellates that they are able to outcompete diatoms during the stratification that follows spring upwelling as they are able to actively hunt and move towards the source of nutrients (Arin et.al, 2007; Ross and Sharples, 2007). This may explain why in the microcosm deplete in both glucose and Si, the autotrophic biomass still increased towards day 8. The increase was due, not to diatoms, but to dinoflagellates.

4.2 Influence of Si

Whilst there was no significant difference between Chl *a* treatments with and without Si, the visual representation (figure 3) shows a distinct difference towards the end of the 8-day experiment. There is a slight increase in Chl *a* after day 6 in the treatment without Si and with glucose however, nothing substantial. The glucose treatment with Si on the other hand (figure 3), showed a drastic increase from day 5 towards day 8. These results would suggest that in the microcosms without glucose addition, diatoms were able to outcompete HB, but only in the presence of Si. Joint, et.al. (2002) conducted a similar experiment in mesocosms to assess the change of phytoplankton assemblages under different nitrate, ammonium, phosphate and silicate addition rates either with or without glucose. They found that the levels of Chl *a* increased over a 6-day period in the mesocosms to which N and P was added with no addition of glucose. However, under the same nutrient conditions in the presence of glucose, the rate of Chl *a* increase was reduced. Furthermore, Joint, et.al. (2002) found that bacterial production increased in the mesocosms containing glucose compared to those with no glucose addition. These results seem to somewhat contradict those of the present study. In the results described previously, the heterotrophic bacteria populations increased rapidly before

decreasing equally as fast, perhaps due to bacterivory, and then increased once more. This was seemingly unaffected by the presence or absence of Si. The growth rate of bacterial populations in the absence of glucose was much slower and more gradual. Interestingly, although it was expected that the bacterial cell counts would remain low in the microcosms with no glucose, there was an increase in the microcosms that contained Si. This coincided with a drop in autotrophic biomass on day 4 and an increase in DOC from day 5 onwards, suggesting that there was remineralisation of the DOC produced and released by the diatom populations. What is more surprising is the fact that this led to greater bacterial abundances than in any other microcosm by almost twice as many in the presence of turbulence.

Havskum, et.al. (2003) conducted an experiment focussing on the impact that varying carbon and silicate levels would have in the presence and absence of N and P on phytoplankton communities. Their results show that under the addition of glucose in NP rich mesocosms, bacterial production increased 2-fold over the first 3 days and continued to rise thereafter. The photosynthetic primary production (PP) in the same mesocosms initially increased but subsequently decreased throughout the remainder of the experiment. Under the same glucose regime with the addition of Si, PP increased significantly whilst bacterial production remained consistently low, albeit still increasing gradually. Of the autotrophs, they found that diatom biomass closely imitated the results of PP and flagellates and cyanobacteria made up a much lower contribution to the autotrophic biomass. This further agrees with the results from the current experiment that the diatoms benefit from a Si replete environment, and that in the presence of glucose, bacterial productivity increases. A point raised in the study by Havskum, et.al.

(2003) is that the bacterial productivity is hindered by the presence of Si due to diatoms being favoured in this environment. Although this is to be expected a priori, it did not appear to be the case in the results from the current study. On the contrary, in the microcosm without glucose and with Si, the bacterial productivity increased whilst the autotrophs increased to begin with but then decreased, which could be explained by a drop in Si on day 4 (figure 7e) in the presence of Si and turbulence and the absence of glucose. Therefore, DOC increased perhaps following higher rates of autotrophic mortality providing the HB with a food source. This is backed up by the fact that following a drop in autotrophic biomass in the presence of Si and absence of glucose, which occurred on day 4 both with and without turbulence (Figure 4c), the DOC concentration increased from day 5 towards the end of the experiment (Figure 4d).

Brzezinski, et.al. (2011) showed that Si is not the only nutrient to limit growth of diatoms. Fe also plays an important role in regulating the uptake rate of silicic acid and the synthesis biogenic silica. This meant that biomass and abundance increased in an environment replete in Fe and Si to a greater extent than an environment replete in Si alone. Whilst this may go some way to explain the reason behind any irregularities in the biomass of diatoms under a Si replete environment in the current study, it is not believed that this will have caused the drop in autotroph abundance occurred in figure 4c. Fe was not measured however if it was influencing the autotrophs to this extent without glucose, it could be assumed that it would have some impact in the experiment with glucose but this was not observed. The current study did not factor in Fe as a co-limiting nutrient and perhaps this would make an interesting area of future research comparing both factors to the presence and absence of

glucose as it appears to play an important role in the development of frustules, controlling the size and thickness.

There was a significant difference in the ratio of diatoms to dinoflagellates between treatments with and without Si, with the former favouring the diatoms. Kremp, et.al. (2008) attributed this to the Si to nitrogen influx ratio. In the case of both studies, this is because of the dependency of diatoms on Si and the rapid growth rate they exhibit under Si replete conditions.

4.3 Competition between HB and Diatoms

The aforementioned assertion that the autochthonous bacteria were remineralising diatom-derived DOC is intriguing and possibly only achievable in a microcosm experiment due to the rapid export of diatom remains from the euphotic zone to the benthos in a natural environment. Or at least enhanced by the retention of said DOC in a microcosm. Wetz and Wheeler (2004) similarly found in microcosm experiments that an accumulation of carbon-rich dissolved organic matter (DOM) coincided with increased abundance and growth rate of bacteria. In this instance they were able to show that this was only true of bacteria which exhibited high nucleic activity (HNA), which was not ascertained in the current study. They found that bacterial activity was stimulated by Chl *a* concentration and not DOC concentration. This would suggest that bacterial activity is stimulated by labile DOC released by phytoplankton or as suggested by Sherr, et.al. (2001), through various food web interactions. Furthermore, as was the case in the current experiment, in the microcosms replete in glucose, Wetz and Wheeler (2004) found a rapid increase in bacterial biomass followed by a subsequent rapid decrease, suggesting this was potentially causes by increased rates of bacterivory and/or viral attacks.

Upon inspection of figure 3.2b and 3.2f showing bacterial cell count in treatments with glucose, with and without Si, respectively, it is clear that the trends in cell count are highly influenced by grazing. Both figures show HB experiencing a rapid increase before a steep decline until day 4. Meanwhile, 3.2c and 3.2g both showed the converse trend in autotroph populations. There was an initial decrease, particularly in the treatment without Si, before a spike on day 4. Grossart and Ploug (2001) showed in their study, which focussed on the breakdown of organic carbon and nitrogen from diatom origin by bacteria, that there was also a high bacterial growth rate on the first day of their experiment. This was then significantly reduced by the second day and the numbers of flagellates and ciliates increased substantially during the third day. Likewise, they attributed this trend to bacterial grazing by populations of protozoans. In their study, Grossart and Ploug (2001) showed that the bacterial growth slowed with degradation of substrate quality which will certainly have exacerbated the bacterial cell reduction rate when paired with protozoan grazing. This will have been less apparent in the current study as nutrients were maintained (continuously resupplied) throughout the experiment. In fact, it is assumed that bacterial growth will have continued at the same rate. Ergo, the dramatic drop in HB on day 4 suggests that phagocytic/heterotrophic/mixotrophic grazing was a key control of HB cell densities. Grossart and Ploug (2001) were investigating microbial degradation of diatom aggregates and so, in their study, nutrients were only added at the start in the form of freeze killed diatoms.

Figure 3.2 b and f showed that bacterial abundance increased once more following the depletion through grazing. The DOC level dropped rapidly at the start and kept consistently low (Figure 3.2d

and f) even though there was a small drop in the autotroph numbers (Figure 3.2 c and g) following the spike on day 4 as discussed previously. This is even more obvious in the study without glucose (Figure 3.3), in which the abundance of bacteria was consistently low. However, in figure 3.3b, where Si was available, there was a slight increase towards the end of the experiment. In coastal environments, bacterial growth rate is expected to be supported by DOC during periods of rapid phytoplankton growth (Vargas, et.al. 2007). Figure 3.3c showed that the cell densities of autotrophs increased primarily before a reduction, which appears to coincide with the increase of HB. Unfortunately, due to missing data, it is difficult to ascertain with any certainty the trend in DOC, however, Vargas, et.al. (2007) found in a study conducted in the Humbolt upwelling system that during the spring diatom bloom, which was closely followed by a bloom of bacteria, the concentrations of DOC were consistently low, which they attributed to a rapid turnover by the bacteria. The same assessment can be made here. In the glucose replete condition, the concentration of DOC was consistently low regardless of cell densities of autotrophs or HB (Figure 3.2). This backs up the results from Vargas et.al. (2007) in highlighting the important coupling between primary production (primary producers) and bacterial biomass (remineralisers). Both bacteria and diatoms rely upon each other to a greater or lesser extent, for nutrients. Neither N or P were ever a limiting factor for either group in any of the microcosm experiments and, in an environment where HB are favoured, grazing will most likely have been the key factor controlling their growth rates. It is highly possible that viral lysis played a role (Vadstein, 2011) but this will have certainly been overshadowed by grazing.

The high level of grazing on HB by the protozoans, flagellates and/or ciliates discussed in this section was so prolific that it could well be attributed to the increase in autotrophic growth in figure 3.3g. This is difficult to assess as the bacteria numbers remained low in the same microcosm (Figure 3.3f) but as seen previously, there is the definite potential for control on the bacteria population and it is speculated here that without bacterivory, the bacterial cell numbers in figure 3.3f would in fact have increased.

4.4 LIMITATIONS OF THE STUDY

Wetz and Weeler (2004) discussed the inherent difficulties in extrapolating results obtained through laboratory studies and applying them to field situations. This will always be the case but does not detract from the importance of lab-based studies. Rather, it highlights the inherent importance as this method of investigation shows when there are other factors impacting an environment to consider, not to mention the cost benefits of lab procedures. The method used in the current study has been used in previous works to obtain results which closely match the behaviour of microbial communities in the real-world oceanic environments (Arin, et.al. 2002; Peters and Gross, 1994; Peters, et.al. 2002; Peters, et.al. 2006).

The use of a x30 conversion factor for Chl *a* to cell carbon content is an issue. This is because autotrophs shall synthesise Chl *a* at different rates largely depending on nutrient availability and/or light levels. The carbon to Chl *a* ratio may vary by about an order of magnitude from 20 to 200, with lower values in nutrient-rich and poorly illuminated environments. As the method used in this study employed a 12:12 light:dark regime and nutrients were constantly added to the microcosms throughout the experiment, it is not thought

that this will have had a great impact on the results as, through the consistency of light and nutrient levels, the Chl *a* production should have been relatively constant over time.

Unfortunately, due to some missing data for various reasons, the final conclusion drawn from the result is not without a degree of uncertainty, however as this was minimal, it can be assumed that the results produced will contribute to improve our understanding of how these microbial plankton communities interact in real-world ocean environments. Unfortunately, due to the time elapsed between sample collection and data analysis, the reasons for the missing data are not known.

The comparatively small volume of microcosms may have stunted the influence of turbulence on the competition between heterotrophic bacteria and diatoms. There may not have been sufficient volume for the nutrients to become depleted in the solution. This combined with the daily addition of nitrogen and phosphorus and the bi-daily addition of silicate in the microcosms to which it was added could have exacerbated this point. At no point during the experiment were the phytoplankton at a nutrient deficit regardless of turbulence. Turbulence did not have a significant impact on the ratio of diatoms to dinoflagellates either, although upon inspection of figure 8, there did seem to be a visual difference. This too, could have been impeded by the low volume of the microcosms and the frequent supply of nutrients.

5 CONCLUSION

The results of the current study have backed up previous work showing that HB benefit from a DOC replete environment whereas diatoms benefit from a Si replete environment. This was to be expected and has a large body of work to support this assertion. Interestingly, however, the expectation that turbulence would further increase the diatom growth rates does not hold for the current study. One argument for this is that because the experiment was conducted in relatively small microcosms, resuspension of the nutrients and increased turbulent shear was not required for the organisms to access the mineral nutrients. It is speculated here that running a similar experiment in a larger microcosm or a mesocosm set up could more accurately represent a natural oceanic environment. Mineral nutrients were added continuously to the microcosms. This was another potential reason that turbulence did not have a significant impact. Turbulent shear will not have been necessary for nutrient diffusion into the diatom cells. It is difficult, therefore, to ascertain the fate of nitrogen and phosphorus depending on turbulence. This still requires further research and is important to shed light on the argument.

The current study simulates the divergent behaviour of microbial plankton communities in contrasting ocean environments. Whereas in permanently stratified ecosystems microbial plankton communities tend to favour the rapid recycling of dissolved organic matter, in coastal upwelling systems, the rapid influx of Redfield nutrient ratios and relative scarcity of dissolved organic carbon would benefit the growth of diatoms. The present study shed light into the competitive dynamics that may occur between diatoms and HB in these contrasting ocean ecosystems.

REFERENCES

Abrantes. F., Cermeño. P., Lopes. C., Romero. O., Matos. L., Iperen. J. V., Rufino. M., Magalhães. V. (2016) Diatoms Si uptake capacity drives carbon export in coastal upwelling systems. *Biogeosciences*, vol. 13, pp. 4099-4109.

Allen. J. T., Brown. L., Sanders. R., Moore. M., Mustard. A., Fielding. S., Lucas. M., Rixen. M., Savidge. G., Henson. S., Mayor. D. (2005) Diatom carbon export enhanced by silicate upwelling in the northeast Atlantic. *Letters*, vol. 437, pp. 728-732.

Amin. S. A., Parker. M. S., Armbrust. E. V. (2012) Interactions between diatoms and bacteria. *Microbiology and Molecular Biology reviews*, vol. 76(3), pp. 667-684.

Arin. L., Marrasé. C., Maar. M., Peters. F., Sala. M. M., Alcaraz. M. (2002) Combined effects of nutrients and small-scale turbulence in a microcosm experiment. I. Dynamics and size distribution of osmotrophic plankton. *Aquatic Microbial Ecology*, vol. 29, pp. 51-61.

Azam. F., Fenchel. T., Field. J. G., Gray. J. S., Mayer-Reil. L. A., Thingstad. F. (1983). The ecological role of water-column microbes in the sea. *Marine Ecological Progress Series*, vol. 10, pp. 257-263.

Bar-On. Y. M., Phillips. R., Milo. R. (2018) The biomass distribution on Earth. *PNAS*, vol. 115(25), pp. 6506-6511.

Barbosa. A. B., Galvão. H. M., Mendes. P. A., Álvarez-Salgado. X. A., Figueiras. F. G., Joint. I. (2001) Short-term variability of heterotrophic bacterioplankton during upwelling off the NW Iberian margin. *Progress in Oceanography*, vol. 51(2-4), pp. 339-359.

Bergvist. J., Klawonn. I., Whitehouse. M. J., Lavik. G., Brüchert. V., Ploug. H. (2018) Turbulence simultaneously stimulates small- and large-scale CO_2 sequestration by chain-forming diatoms in the sea. *Nature Communications*, vol. 9(1), pp. 1-10.

Bjørnsen. P. K. (1986) Automatic determination of bacterioplankton biomass by image analysis. *Applied and Environmental Microbiology*, vol. 51(6), pp. 1199-1204.

Bratbak. G., Thingstad. T. F. (1985) Phytoplankton-bacteria interactions: an apparent paradox? Analysis of a model system with both competition and commensualism. *Marine Ecology Progress Series*, vol. 25, pp. 23-30.

Brzezinski. M. A., Baines. S. B., Balch. W. M., Beucher. C. P., Chai. F., Dugdale. R. C., Krause. J. W., Landry. M. R., Marchi. A., Measures. C. I., Nelson. D. M., Parker. A. E., Poulton. A. J., Selph. K. E., Strutton. P. G., Taylor. A. G., Twining. B. S. (2011) Co-limitation of diatoms by iron and silicic acid in the equatorial Pacific. *Deep-Sea Research II*, vol. 28, pp. 493-511.

Cavicchioli. R., Ripple. W. J., Timmis. K. N., Azam. F., Bakken. L. R., Baylis. L. R., Behrenfeld. M. J., Boetius. L. R., Boyd. P. W., Classen. A. T., Crowther. T. W., Danovaro. R., Foreman. C. M., Huisman. J., Hutchins. D. A., Jansson. J. K., Karl. D. M., Koskella. B., Welch. D. B. M., Martiny. J. B. H., Moran. M. A., Orphan. V. J., Reay. D. S., Remais. J. V., Rich. V. I., Singh. B. K., Stein. L. Y., Stewart. F. J., Sullivan. M. B., van Oppen. M. J. H., Weaver. S. C., Webb. E. A., Webster. N. S. (2019) Scientists' warning to humanity: microorganisms and climate change. *Nature Reviews – Microbiology*, vol. 17, pp. 569-586.

Chrzanowski. T. H., Sterner. R. W., Elser. J. J. (1995) Nutrient enrichment and nutrient regeneration stimulate bacterioplankton growth. *Microbial Ecology*, vol. 29, pp. 221-230.

Diner. R. E., Schwenk. S. M., McCrow. J. P., Zheng. H., Allen. A. E. (2016) Genetic manipulation of competition for nitrate between heterotrophic bacteria and diatoms. *Frontiers in Microbiology*, vol. 7(880), pp. 1-16.

Drakare. S. (2002) Competition between picoplanktonic cyanobacteria and heterotrophic bacteria along crossed gradients of glucose and phosphate. *Microbial Ecology*, vol. 44, pp. 327-335.

Dugdale. R. C., Wilkerson. F. P. (2001) Sources and fates of silicon in the oceans: the role of diatoms in the climate and glacial cycles. *Scientia Marina*, vol. 65(2), pp. 141-152.

Egge. R. C., Aksnes. D. L. (1992) Silicate as regulating nutrient in phytoplankton competition. *Marine Ecology Progress Series*, vol. 83, pp. 281-289.

Fatima. A., Cermeño. P., Lopes. C., Romero. O., Matos. L., Iperen. J. V., Rufino. M., Magalhães. V. (2016) Diatom Si uptake capacity drives carbon export in coastal upwelling systems. *Biogeosciences*, vol. 13, pp. 4099-4109.

Gasol. J. M., Giorgio. P. A. D. (2000) Using flow cytometry for counting natural planktonic bacteria and understanding the structure of planktonic communities. *Scientia Marina*, vol. 64(2), pp. 197-224.

Gibson. C. H. (2000) Laboratory and ocean studies of phytoplankton response to fossil turbulence. *Dynamics of Atmospheres and Oceans*, vol. 31, pp. 295-306.

Grasshoff. P. (1983) Methods of seawater analysis. Verlag Chemie. *FRG*, vol. 419, pp. 61-72.

Grossart. H. P., Ploug. H. (2001) Microbial degradation of organic carbon and nitrogen on diatom aggregates. *American Society of Limnology and Oceanography*, vol. 46(2), pp. 267-277.

Guerrini. F., Mazzotti. A., Boni. L., Pistocchi. R. (1998) Bacterial-algal interactions in polysaccharide production. *Aquatic Microbial Ecology*, vol. 15, pp. 247-253.

Havskum. H., Thingstad. T. F., Scharek. R., Peters. F., Berdalet. E., Sala. M. M., Alcaraz. M., Bangsholt. J. C., Zweifel. U. L., Hagström. Å., Perez. M., Dolan. J. R. (2003) Silicate and labile DOC interfere in structuring the microbial food web via algal-bacterial competition for mineral nutrients: Results of a mesocosm experiment. *The American Society of Limnology and Oceanography*, vol. 48(1), pp. 129-140.

Huisman. J., Sharples. J., Stroom. J. M., Visser. P. M., Edwin. W., Kardinaal. A., Verspagen. J. M. H., Sommeijer. B. (2004) Changes in turbulent mixing shift competition for light between phytoplankton species. *Ecology*, vol. 85(11), pp. 2960-2970.

Joint. I., Henriksen. P., Fonnes. G. A., Bourne. D., Thingstad. T. F., Reimann. B. (2002) Competition for inorganic nutrients between phytoplankton in nutrient manipulated mesocosms. *Aquatic Microbial Ecology*, vol. 29, pp. 145-159.

Kana. T. M., Gilbert. P. M. (1987) Effects of irradiances on up to 2000 μE m^{-2} s^{-1} on marine *Synochoccus* WH7803-I. Growth, pigmentation, and cell composition. *Deep Sea Research Part A. Oceanographic Research Papers*, vol. 34(4), pp. 479-495.

Kirchman. D. L. (1994) The uptake of inorganic nutrients by heterotrophic bacteria. *Microbial Ecology*, vol. 28, pp. 255-271.

Kremp. A., Tmminen. T., Spilling. K. (2008) Dinoflagellate bloom formation in natural assemblages with diatoms: nutrient competition and growth strategies in Baltic spring phytoplankton. *Aquatic Microbial Ecology*, vol. 50, pp. 181-196.

Montagnes. D. J. S., Berges. J. A., Harrison. P. J., Taylor. F. J. R. (1994) Estimating carbon, nitrogen, protein, and chlorophyll *a* from volume in marine phytoplankton. *American Society of Limnology and Oceanography*, vol. 39(5), pp. 1044-1060.

Mouriño-Carballido. B., Agustí. S., Bode. A., Cermeño. P., Chouciño. P., Silva. J., Fernàndez-Castro. B., Gasol. J., Gilcoto. M., Graña. R., Latasa. M., Lubiàn. L., Marañón. E., Moran. X. A. G., Moreno-Ostos. E., Moreira-Coello. V., Otero-Ferrer. J. L., Ruiz. M., Scharek. R., Callina. S., Varela. M., Villamaña. M. (2016) Control of the structure of phytoplankton communities by turbulence and nutrient supply dynamics (CHAOS).

Peters. F., Arin. L., Marrasé. C., Berdalet. E., Sala. M. M. (2006) Effects of small-scale turbulence on the growth of two diatoms of different size in a phosphorus-limiting medium. *Journal of Marine Systems*, vol. 61, pp. 134-148.

Peters. F., Gross. T. (1994) Increase grazing rates of microplankton in response to small-scale turbulence. *Marine Ecology Progress Series*, vol. 115, pp. 299-307.

Peters. F., Marrasé. C., Havskum. H., Rassoulzadegan. F., Dolan. J., Alcaraz. M., Gasol. J. M. (2002) Turbulence and the microbial food web: effects on bacterial losses to predation and on

community structure. *Journal of Plankton Research*, vol. 4(4), pp. 321-331.

Porter. K. G., Feig. Y. S. (1980) The use of DAPI for identifying and counting aquatic microflora 1. *The American Society of Limnology and Oceanography*, vol. 25(5), pp. 943-948.

Ribes. M., Coma. R., Gili. J. M. (1999) Heterogenous feeding in benthic suspension feeders: the natural diet and grazing rate of the temperate gorgonian *Paramuricea clavate* (Cnidaria: Octorallia) over a year cycle. *Marine Ecology Progress Series*, vol. 183, pp. 125-137.

Ross. O. N., Sharples. J. (2007) Phytoplankton motility and the competition for nutrients in the thermocline. *Marine Ecology Progress Series*, vol. 347, pp. 21-38.

Rynearson. T. A., Richardson. K., Limpitt. R. S., Sieracki. M. E., Poulton. A. B., Lyngsgaard. M. M., Perry. M. J. (2013) Major contribution of diatom resting spores to vertical flux in the sub-polar north Atlantic. *Deep-Sea Research I*, vol. 82, pp. 60-71.

Sala. M. M., Peters. F., Gasol. J. M., Pedrós-Alió. C., Marrasé. C., Vaqué. D. (2002) Seasonal and spatial variations in the nutrient limitation of bacterioplankton growth in the northwestern Mediterranean. *Aquatic Microbial Ecology*, vol. 27, pp. 47-56.

Sherr. E. B., Sherr. B. F., Cowles. T. J. (2001) Mesoscale variability in bacterial activity in the Northern Pacific Ocean off Oregon, USA. *Aquatic Microbial Ecology*, vol. 25, pp. 21-30.

Thingstad. T. F., Havskum. H., Zweifel. U. L., Berdalet. E., Sala. M. M., Peters. F., Alcaraz. M., Scharek. R., Perez. M., Jaquet. S., Flaten. G. A. F., Dolan. J. R., Marrasé. C., Rassoulzadegan. F., Hagstrøm. A., Vaulot. D. (2007) Ability of a “minimum” microbial

food web model to reproduce response patterns observed in mesocosms manipulated with N and P, glucose, and Si. *Journal of Marine Systems*, vol. 64, pp. 15-34.

Utermöhl. H. (1958) To the perfection of quantitative phytoplankton methodology. *Mitt Int Ver Theor Angew Limnol*, vol. 9, pp. 1-38.

Vadstein. O. (2011) Large variation in growth-limiting factors for marine heterotrophic bacteria in the Arctic waters of Spitsbergen (78°N). *Aquatic Microbial Ecology*, vol. 63, pp. 289-297.

Vargas. C. A., Martinez. R. A., Cuevas. L. A., Paves. M. A., Cartes. C., González. H. E., Escribano. R., Daneri. G. (2007) The relative importance of microbial and classical food webs in a highly productive coastal upwelling area. *American Society of Limnology and Oceanography*, vol. 52(4), pp. 1495-1510.

Verity. P. G., Robertson. C. Y., Tronzo. C. R., Andrews. M. G., Nelson. J. R., Sieracki. M. E. (1992) Relationships between cell volume and the carbon and nitrogen content of marine photosynthetic nanoplankton. *American Society of Limnology and Oceanography*, vol. 37(7), pp. 1434-1446.

Wetz. M. S., Wheeler. P. A. (2004) Response of bacteria to simulated upwelling phytoplankton blooms. *Marine Ecological Progress*, vol. 272, pp. 49-57.

APPENDICES

Table of normality tests

		Shapiro-Wilk		
Subject	Condition	Statistic	p-value	Outcome
Chl a	Glucose	0.918	0.375	Fail to reject H0
	Glucose and Turbulance	0.797	0.019	Reject H0
	Glucose and Si	0.74	0.004	Reject H0
	Glucose, Si and Turbulence	0.552	0	Reject H0
	Control	0.768	0.009	Reject H0
	Si	0.956	0.757	Fail to reject H0
	Turbulence	0.754	0.006	Reject H0
	Si and Turbulence	0.921	0.399	Fail to reject H0
Bacterial cell count	Glucose	0.951	0.704	Fail to reject H0
	Glucose and Turbulence	0.976	0.943	Fail to reject H0
	Glucose and Si	0.969	0.883	Fail to reject H0
	Glucose, Si and Turbulence	0.897	0.392	Fail to reject H0
	Control	0.909	0.31	Fail to reject H0
	Si	0.866	0.112	Fail to reject H0
	Turbulence	0.946	0.646	Fail to reject H0
	Si and Turbulence	0.818	0.033	Reject H0
A/(A+HB)	Glucose	0.764	0.012	Reject H0
	Glucose and Turbulence	0.875	0.14	Fail to reject H0
	Glucose and Si	0.866	0.212	Fail to reject H0
	Glucose, Si and Turbulence	0.753	0.009	Reject H0
	Control	0.962	0.822	Fail to reject H0
	Si	0.908	0.301	Fail to reject H0
	Turbulence	0.967	0.867	Fail to reject H0
	Si and Turbulence	0.905	0.285	Fail to reject H0
DOC	Glucose	0.907	0.299	Fail to reject H0
	Glucose and Turbulence	0.801	0.021	Reject H0
	Glucose and Si	0.962	0.819	Fail to reject H0
	Glucose, Si and Turbulence	0.936	0.538	Fail to reject H0
	Control	0.89	0.273	Fail to reject H0
	Si	0.932	0.538	Fail to reject H0
	Turbulence	0.944	0.672	Fail to reject H0
	Si and Turbulence	0.963	0.834	Fail to reject H0

APPENDIX I – Shapiro-Wilk test for all variables with outcome, test statistic, p-value and the decision as to whether to accept or reject null hypothesis (H0).

Statistics

Subject	Condition	Standard deviation	Variance	Mean
Chl a	Glucose	0.534	0.285	1.277
	Glucose and Turbulence	0.912	0.831	1.666
	Glucose and Si	2.84	8.067	3.058
	Glucose, Si and Turbulence	12.616	159.17	7.294
	Control	1.456	0.121	1.96
	Si	2.541	6.458	4.224
	Turbulence	1.118	1.249	2.1
	Si and Turbulence	5.292	28.004	6.738
Bacterial cell count	Glucose	1527485.663	2.33321E+12	2615076.687
	Glucose and Turbulence	1660855.17	2.75844E+12	3465470.882
	Glucose and Si	1381366.275	1.90817E+12	2581785.7
	Glucose, Si and Turbulence	2323597.742	5.39911E+12	3329988.228
	Control	970700.493	9.42259E+11	1863620.103
	Si	1637432.819	2.68119E+12	2366017.512
	Turbulence	839799.701	7.05264E+11	1780683.222
	Si and Turbulence	3828914.015	1.46606E+13	4130817.885
A/(A+HB)	Glucose	0.475	0.226	1.58
	Glucose and Turbulence	0.378	0.143	1.798
	Glucose and Si	0.541	0.292	1.654
	Glucose, Si and Turbulence	0.406	0.164	1.744
	Control	0.144	0.021	0.559
	Si	0.125	0.016	0.688
	Turbulence	0.136	0.018	0.6
	Si and Turbulence	0.134	0.018	0.664
DOC	Glucose	18.864	355.861	41.889
	Glucose and Turbulence	19.445	378.861	39.889
	Glucose and Si	17.146	294	54.333
	Glucose, Si and Turbulence	27.078	579.75	53.333
	Control	0.129	0.017	1.214
	Si	0.082	0.007	1.229
	Turbulence	0.165	0.027	1.344
	Si and Turbulence	0.178	0.032	1.324

APPENDIX II – Statistics for all variables including the standard deviation, the variance and the mean for each condition

Chlorophyll a

Test	Test statistic	DF	p-value
Bartlett's K-squared	106.63	7	<2.2E-16
Kruskal-Wallis chi-squared	18.339	7	0.01053

Dunn test with Bonferroni adjustment

Comparison	Z value	p-value	p-adjusted
Control - Glucose	0.822809	0.4106	1
Control - Glucose + Si	-0.811538	0.4171	1
Glucose - Glucose + Si	-1.634346	0.1022	1
Control - Glucose + Si + Turbulence	-1.741424	0.0816	1
Glucose - Glucose + Si + Turbulence	-2.564233	0.0103	0.28953
Glucose + Si - Glucose + Si + Turbulence	-0.929887	0.3524	1
Control - Glucose + Turbulence	0.011271	0.991	1
Glucose - Glucose + Turbulence	-0.811538	0.4171	1
Glucose + Si - Glucose + Turbulence	0.822809	0.4106	1
Glucose + Si + Turbulence - Glucose + Turbulence	1.752696	0.0797	1
Control - Si	-2.1641	0.0305	0.85279
Glucose - Si	-2.986909	0.0028	0.07891
Glucose + Si - Si	-1.352563	0.1762	1
Glucose + Si + Turbulence - Si	-0.422676	0.6725	1
Glucose + Turbulence - Si	-2.175371	0.0296	0.82886
Control - Si + Turbulence	-2.389527	0.0169	0.47236
Glucose - Si + Turbulence	-3.212336	0.0013	0.03686
Glucose + Si - Si + Turbulence	-1.57799	0.1146	1
Glucose+ Si + Turbulence - Si + Turbulence	-0.648103	0.5169	1
Glucose + Turbulence - Si + Turbulence	-2.400799	0.0164	0.45806
Si - Si + Turbulence	-0.225427	0.8216	1
Control - Turbulence	-0.715731	0.4742	1
Glucose - Turbulence	-1.53854	0.1239	1
Glucose + Si - Turbulence	0.095807	0.9237	1
Glucose + Si + Turbulence - Turbulence	1.025693	0.305	1
Glucose + Turbulence - Turbulence	-0.727002	0.4672	1
Si - Turbulence	1.448369	0.1475	1
Si + Turbulence - Turbulence	1.673796	0.0942	1

Appendix III – List of results for Bartlett's K-squared test, Kruskal-Wallis test and Dunn test with Bonferroni adjustment for *Chlorophyll a* data.

Heterotrophic Bacteria

Test	Test statistic	DF	p-value
Bartlett's K-squared	25.897	7	0.00053
Kruskal-Wallis chi-squared	8.392	7	0.2993

Dunn test with Bonferroni adjustment

Comparison	Z value	p-value	p-adjusted
Control - Glucose	-1.049519	0.2939	1
Control - Glucose + Si	-1.27612	0.2019	1
Glucose - Glucose + Si	-0.226601	0.8207	1
Control - Glucose + Si + Turbulence	-1.368811	0.1711	1
Glucose - Glucose + Si + Turbulence	-0.481805	0.6299	1
Glucose + Si - Glucose + Si + Turbulence	-0.290293	0.7716	1
Control - Glucose + Turbulence	-2.110964	0.0348	0.97371
Glucose - Glucose + Turbulence	-1.061445	0.2885	1
Glucose + Si - Glucose + Turbulence	-0.834845	0.4038	1
Glucose + Si + Turbulence - Glucose + Turbulence	-0.41528	0.6779	1
Control - Si	-0.524759	0.5998	1
Glucose - Si	0.524759	0.5998	1
Glucose + Si - Si	0.75136	0.4524	1
Glucose + Si + Turbulence - Si	0.925308	0.3548	1
Glucose + Turbulence - Si	1.586205	0.1127	1
Control - Si + Turbulence	-1.717395	0.0859	1
Glucose - Si + Turbulence	-0.667876	0.5042	1
Glucose + Si - Si + Turbulence	-0.441275	0.659	1
Glucose + Si + Turbulence - Si + Turbulence	-0.082653	0.9341	1
Glucose + Turbulence - Si + Turbulence	0.39357	0.6939	1
Si - Si + Turbulence	-1.192635	0.233	1
Control - Turbulence	-0.035779	0.9715	1
Glucose - Turbulence	1.01374	0.3107	1
Glucose + Si - Turbulence	1.240341	0.2148	1
Glucose + Si + Turbulence - Turbulence	1.338572	0.1807	1
Glucose + Turbulence - Turbulence	2.075185	0.038	1
Si - Turbulence	0.48898	0.6249	1
Si + Turbulence - Turbulence	1.681615	0.0926	1

Appendix IV – List of results for Bartlett's K-squared test, Kruskal-Wallis test and Dunn test with Bonferroni adjustment for heterotrophic bacteria data.

Autotroph:(Autotroph + Heterotrophic Bacteria) Ratio

Test	Test statistic	DF	p-value
Bartlett's K-squared	70.691	7	1.07E-12
Kruskal-Wallis chi-squared	50.33	7	1.24E-08

Dunn test with Bonferroni adjustment

Comparison	Z value	p-value	p-adjusted
Control - Glucose	3.0300431	2.45E-03	0.068465
Control - Glucose + Si	2.2640843	2.36E-02	0.65993
Glucose - Glucose + Si	-0.7659589	4.44E-01	1
Control - Glucose + Si + Turbulence	2.4105176	1.59E-02	0.446037
Glucose - Glucose + Si + Turbulence	-0.6195255	5.36E-01	1
Glucose + Si - Glucose + Si + Turbulence	0.1464333	8.84E-01	1
Control - Glucose + Turbulence	3.2102687	1.33E-03	0.037131
Glucose - Glucose + Turbulence	0.1802256	8.57E-01	1
Glucose + Si - Glucose + Turbulence	0.9461845	3.44E-01	1
Glucose + Si + Turbulence - Glucose + Turbulence	0.7997512	4.24E-01	1
Control - Si	-1.2953716	1.95E-01	1
Glucose - Si	-4.3254147	1.52E-05	0.000426
Glucose + Si - Si	-3.5594559	3.72E-04	0.010405
Glucose + Si + Turbulence - Si	-3.7058892	2.11E-04	0.005898
Glucose + Turbulence - Si	-4.5056403	6.62E-06	0.000185
Control - Si + Turbulence	-1.0250332	3.05E-01	1
Glucose - Si + Turbulence	-4.0550763	5.01E-05	0.001403
Glucose + Si - Si + Turbulence	-3.2891174	1.01E-03	0.028141
Glucose + Si + Turbulence - Si + Turbulence	-3.4355508	5.91E-04	0.016558
Glucose + Turbulence - Si + Turbulence	-4.2353019	2.28E-05	0.000639
Si - Si + Turbulence	0.2703384	7.87E-01	1
Control - Turbulence	-0.4843563	6.28E-01	1
Glucose - Turbulence	-3.5143995	4.41E-04	0.012341
Glucose + Si - Turbulence	-2.7484406	5.99E-03	0.167663
Glucose + Si + Turbulence - Turbulence	-2.8948739	3.79E-03	0.106207
Glucose + Turbulence - Turbulence	-3.6946251	2.20E-04	0.006166
Si - Turbulence	0.8110153	4.17E-01	1
Si + Turbulence - Turbulence	0.5406768	5.89E-01	1

Appendix V – List of results for Bartlett's K-squared test, Kruskal-Wallis test and Dunn test with Bonferroni adjustment for Autotroph:(Autotroph + Heterotrophic Bacteria) Ratio data.

Dissolved Organic Carbon

Test	Test statistic	DF	p-value
Bartlett's K-squared	32.273	7	3.61E-05
Kruskal-Wallis chi-squared	27.948	7	0.000225

Dunn test with Bonferroni adjustment

Comparison	Z value	p-value	p-adjusted
Control - Glucose	-1.980942	0.0476	1
Control - Glucose + Si	-1.977746	0.048	1
Glucose - Glucose + Si	-0.139024	0.8894	1
Control - Glucose + Si + Turbulence	-3.360236	0.0008	0.021805
Glucose - Glucose + Si + Turbulence	-1.427705	0.1534	1
Glucose + Si - Glucose + Si + Turbulence	-1.182774	0.2369	1
Control - Glucose + Turbulence	-3.696147	0.0002	0.006129
Glucose - Glucose + Turbulence	-1.723454	0.0848	1
Glucose + Si - Glucose + Turbulence	-1.446489	0.148	1
Glucose + Si + Turbulence - Glucose + Turbulence	-0.254358	0.7992	1
Control - Si	-0.045913	0.9634	1
Glucose - Si	2.002945	0.0452	1
Glucose + Si - Si	1.993391	0.0462	1
Glucose + Si + Turbulence - Si	3.43065	0.0006	0.01686
Glucose + Turbulence - Si	3.784468	0.0002	0.004313
Control - Si + Turbulence	-1.031219	0.3024	1
Glucose - Si + Turbulence	1.040412	0.2981	1
Glucose + Si - Si + Turbulence	1.10167	0.2706	1
Glucose + Si + Turbulence - Si + Turbulence	2.509508	0.0121	0.338518
Glucose + Turbulence - Si + Turbulence	2.848928	0.0044	0.122827
Si - Si + Turbulence	-1.020602	0.3074	1
Control - Turbulence	-1.178052	0.2388	1
Glucose - Turbulence	0.764255	0.4447	1
Glucose + Si - Turbulence	0.845911	0.3976	1
Glucose + Si + Turbulence - Turbulence	2.143549	0.0321	0.897933
Glucose + Turbulence - Turbulence	2.446635	0.0144	0.403751
Si - Turbulence	-1.170774	0.2417	1
Si + Turbulence - Turbulence	-0.218294	0.8272	0

Appendix VI – List of results for Bartlett's K-squared test, Kruskal-Wallis test and Dunn test with Bonferroni adjustment for dissolved organic carbon data.

(a)

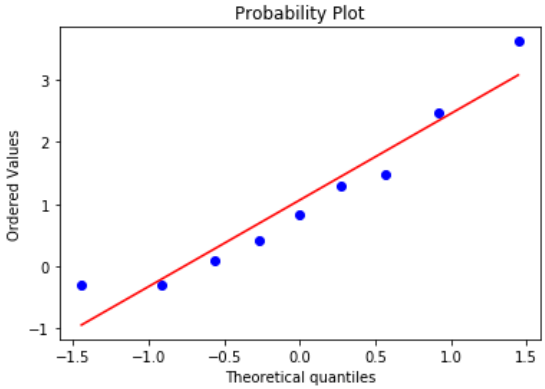
Probability Plot
Ordered Values
Theoretical quantiles

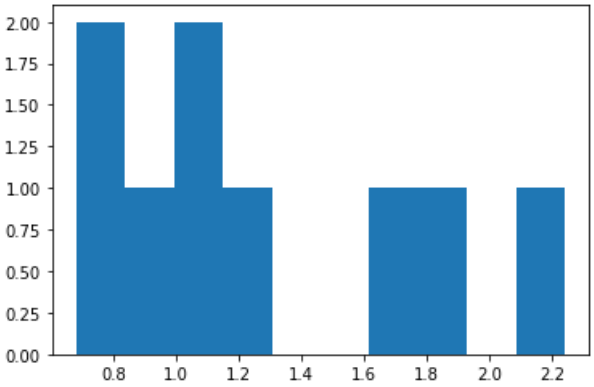

(b)

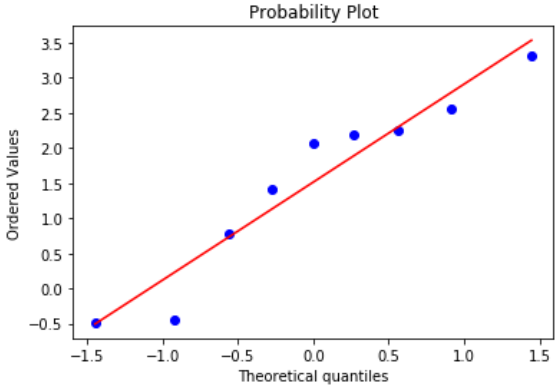
Probability Plot
Ordered Values
Theoretical quantiles

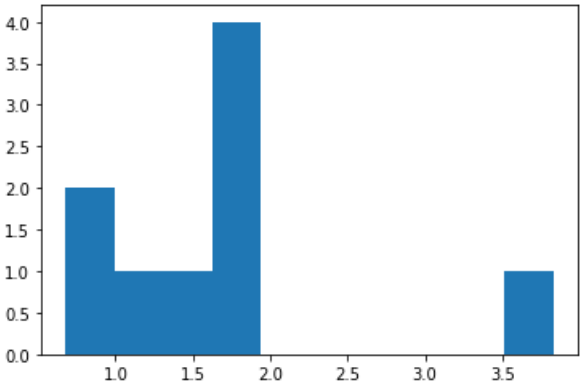

(c)

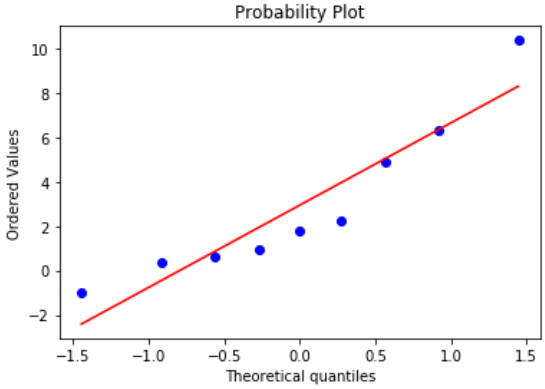
Probability Plot
Ordered Values
Theoretical quantiles

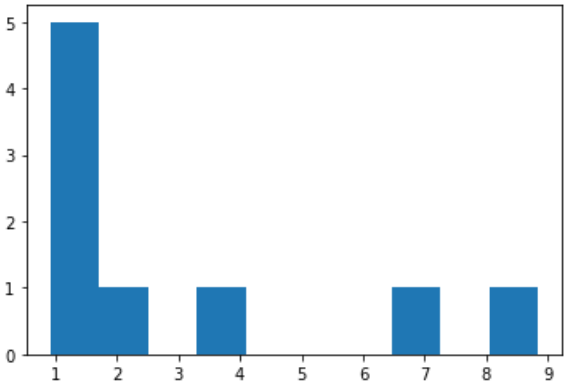

(d)

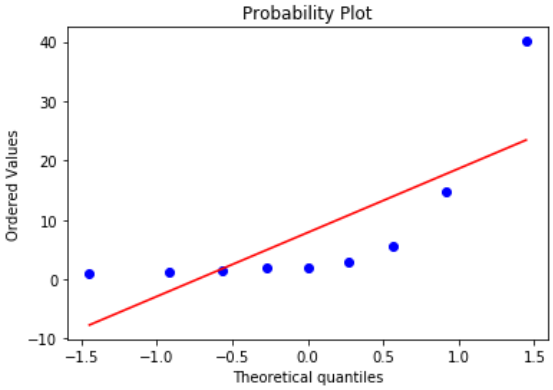
Probability Plot
Ordered Values
Theoretical quantiles

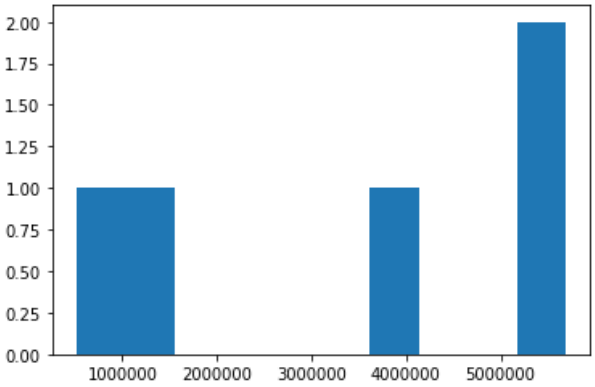
1000000
2000000
3000000
4000000
5000000

(e)

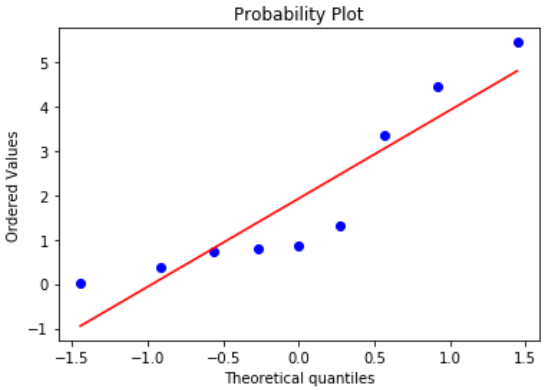
Probability Plot
Ordered Values
Theoretical quantiles

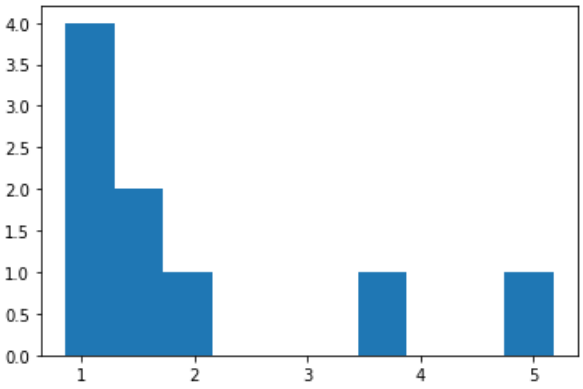

(f)

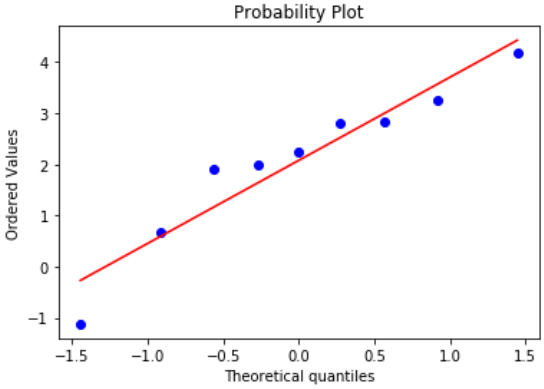
Probability Plot
Ordered Values
Theoretical quantiles

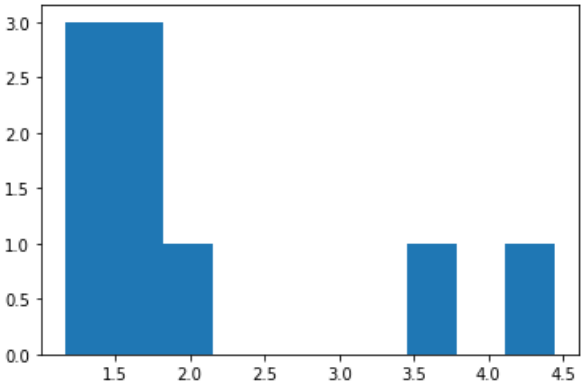

(g)

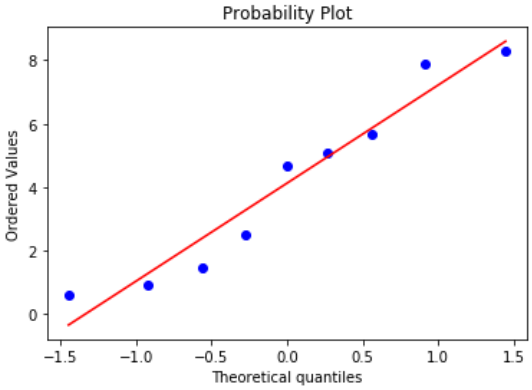

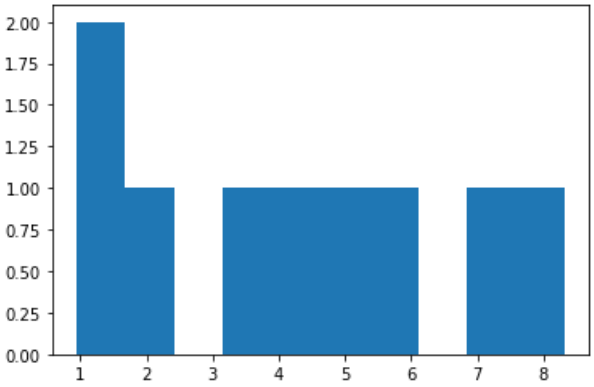

(h)

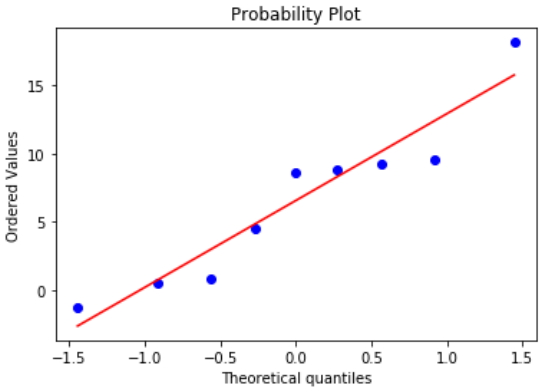

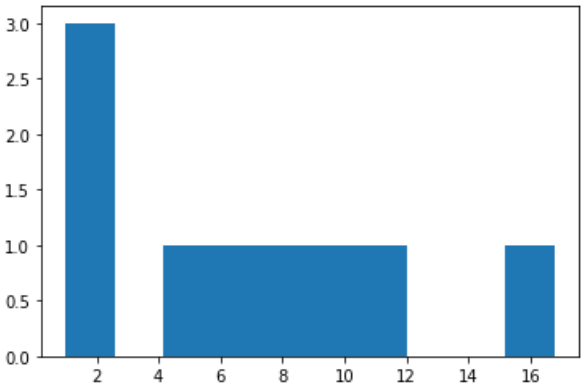

APPENDIX VII – Visual representations of normality displayed as Q-Q plots and histograms to visualise distribution for *Chlorophyll a* for; (a) glucose; (b) glucose and turbulence; (c) glucose and silicate; (d) glucose, silicate and turbulence; (e) control; (f) turbulence; (g) silicate; (h) silicate and turbulence.

(a)

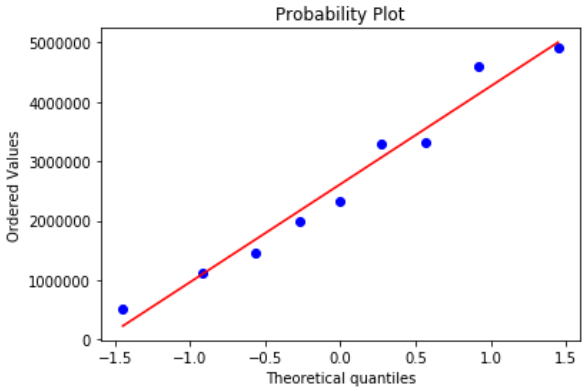
Probability Plot
Ordered Values
Theoretical quantiles
5000000
4000000
3000000
2000000
1000000
0
−1.5
−1.0
−0.5
0.0
0.5
1.0
1.5

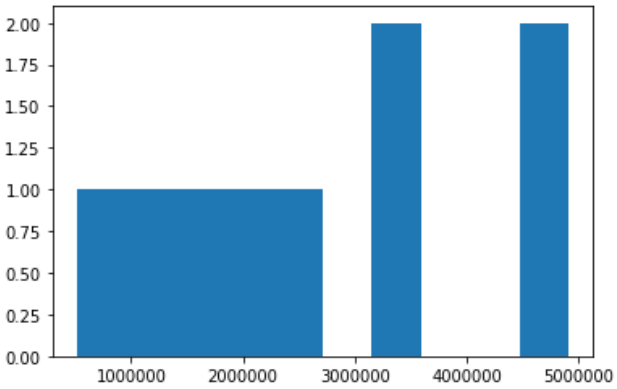
2.00
1.75
1.50
1.25
1.00
0.75
0.50
0.25
0.00
1000000
2000000
3000000
4000000
5000000

(b)

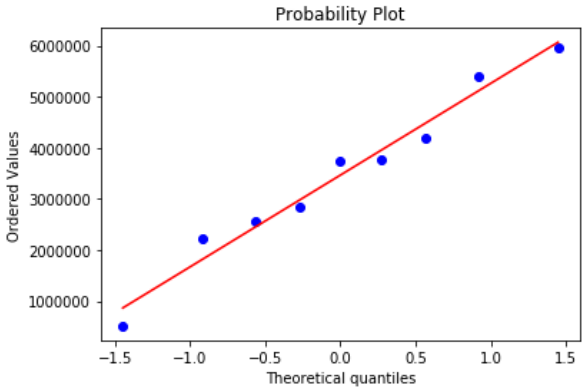
Probability Plot
Ordered Values
Theoretical quantiles
6000000
5000000
4000000
3000000
2000000
1000000
−1.5
−1.0
−0.5
0.0
0.5
1.0
1.5

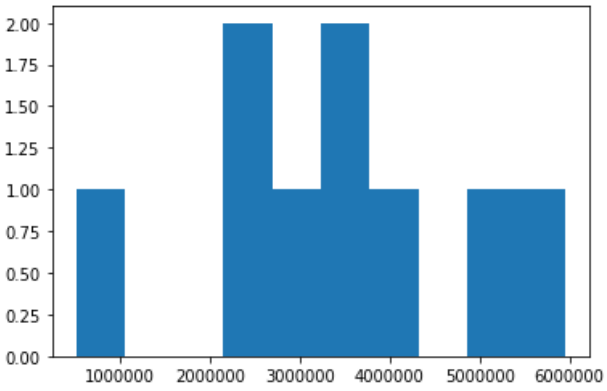
2.00
1.75
1.50
1.25
1.00
0.75
0.50
0.25
0.00
1000000
2000000
3000000
4000000
5000000
6000000

(c)

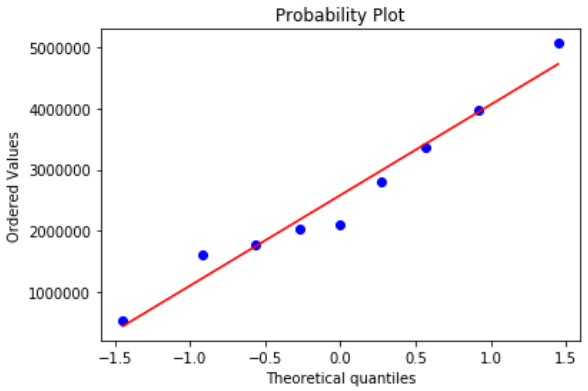
Probability Plot
Ordered Values
Theoretical quantiles
5000000
4000000
3000000
2000000
1000000
−1.5
−1.0
−0.5
0.0
0.5
1.0
1.5

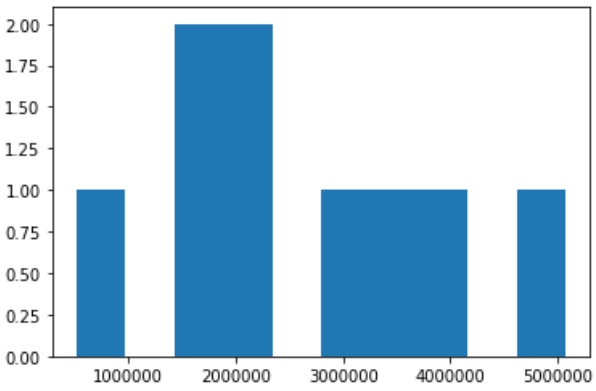
2.00
1.75
1.50
1.25
1.00
0.75
0.50
0.25
0.00
1000000
2000000
3000000
4000000
5000000

(d)

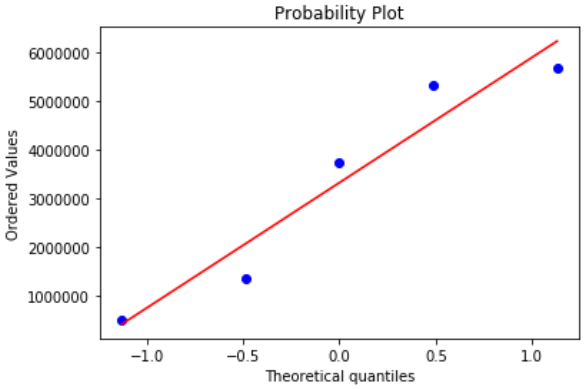
Probability Plot
Ordered Values
Theoretical quantiles
6000000
5000000
4000000
3000000
2000000
1000000
−1.0
−0.5
0.0
0.5
1.0

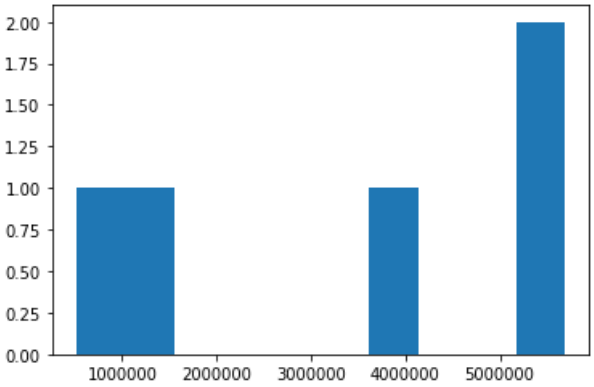
2.00
1.75
1.50
1.25
1.00
0.75
0.50
0.25
0.00
1000000
2000000
3000000
4000000
5000000

(e)

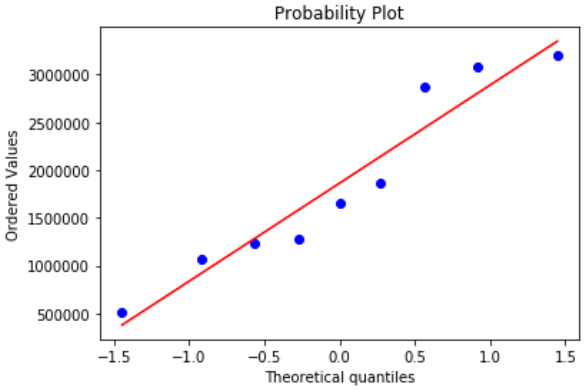
Probability Plot
Ordered Values
Theoretical quantiles
3000000
2500000
2000000
1500000
1000000
500000
−1.5
−1.0
−0.5
0.0
0.5
1.0
1.5

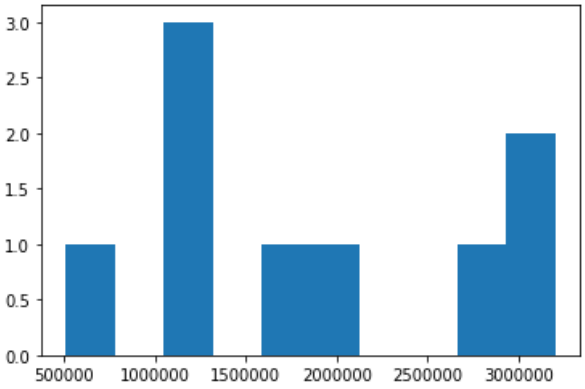
3.0
2.5
2.0
1.5
1.0
0.5
0.0
500000
1000000
1500000
2000000
2500000
3000000

(f)

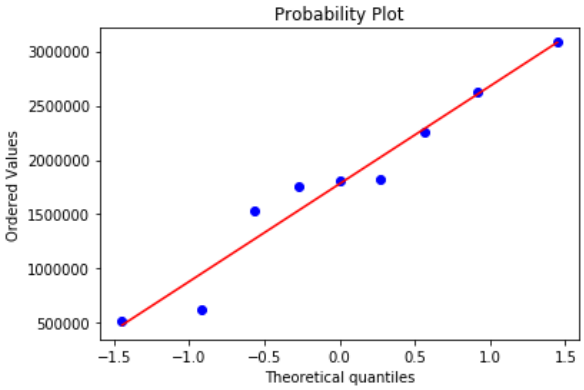
Probability Plot
Ordered Values
Theoretical quantiles
3000000
2500000
2000000
1500000
1000000
500000
−1.5
−1.0
−0.5
0.0
0.5
1.0
1.5

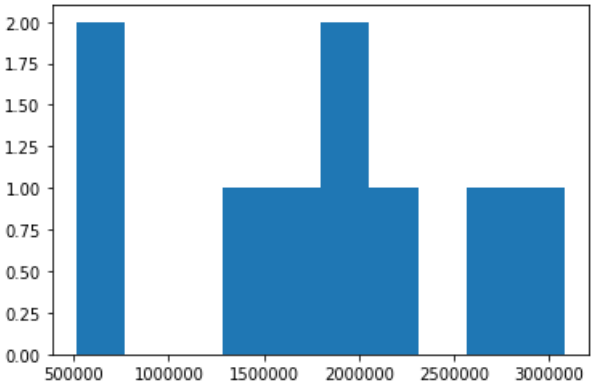
2.00
1.75
1.50
1.25
1.00
0.75
0.50
0.25
0.00
500000
1000000
1500000
2000000
2500000
3000000

(g)

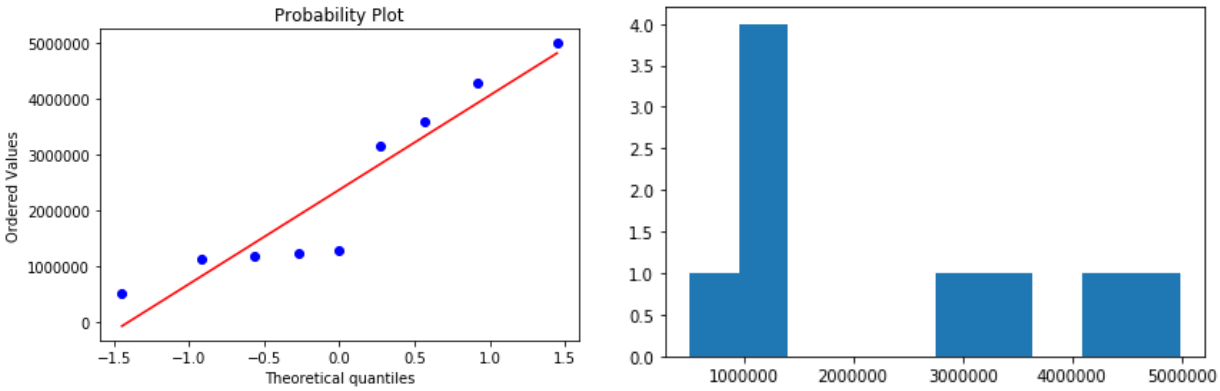

(h)

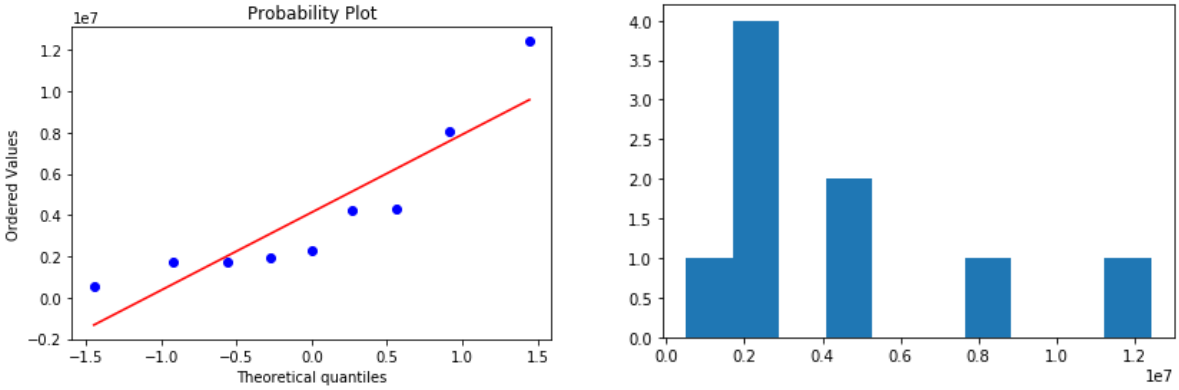

APPENDIX VIII - Visual representations of normality displayed as Q-Q plots and histograms to visualise distribution for bacterial cell count for; (a) glucose; (b) glucose and turbulence; (c) glucose and silicate; (d) glucose, silicate and turbulence; (e) control; (f) turbulence; (g) silicate; (h) silicate and turbulence.

(a)

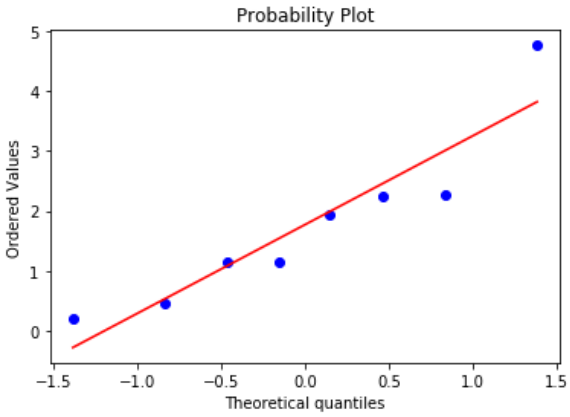
Probability Plot
Ordered Values
Theoretical quantiles

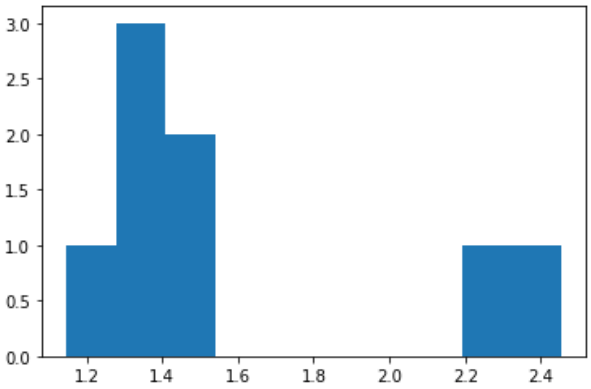

(b)

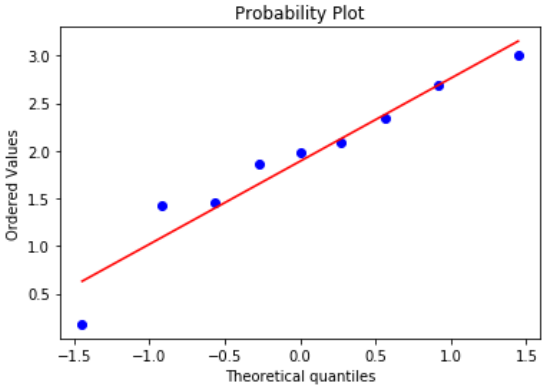
Probability Plot
Ordered Values
Theoretical quantiles

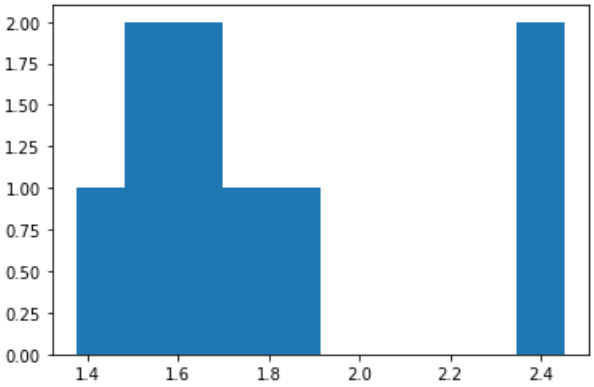

(c)

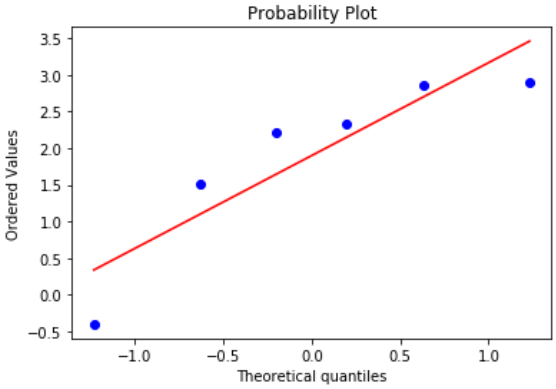
Probability Plot
Ordered Values
Theoretical quantiles

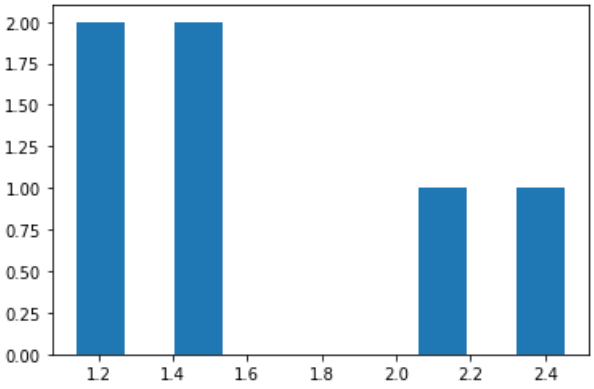

(d)

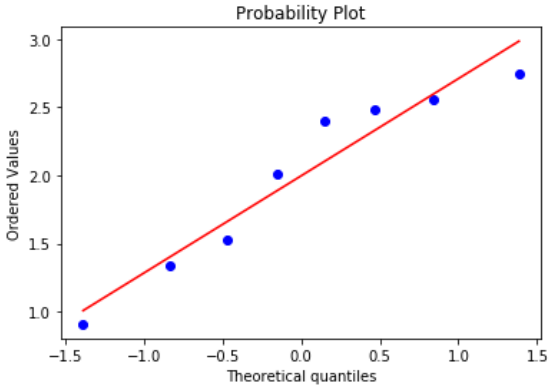
Probability Plot
Ordered Values
Theoretical quantiles

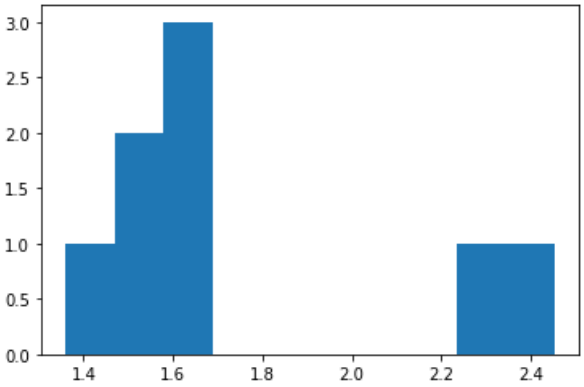

(e)

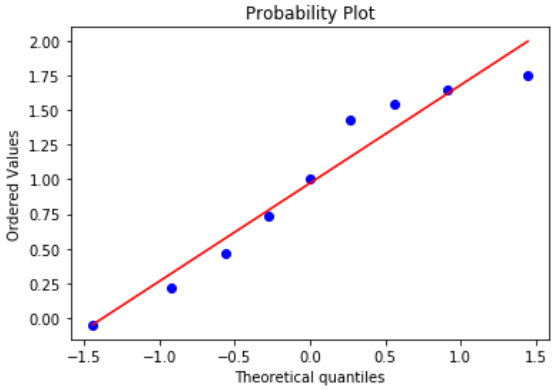
Probability Plot
Ordered Values
Theoretical quantiles

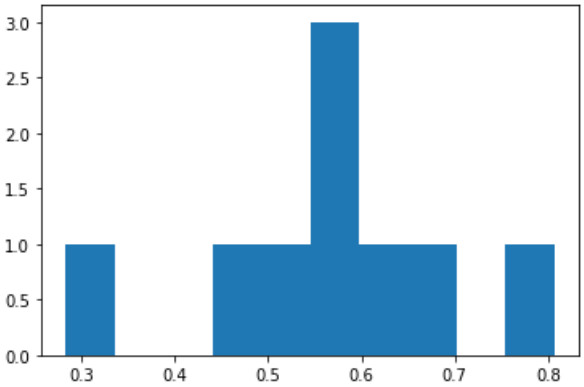

(f)

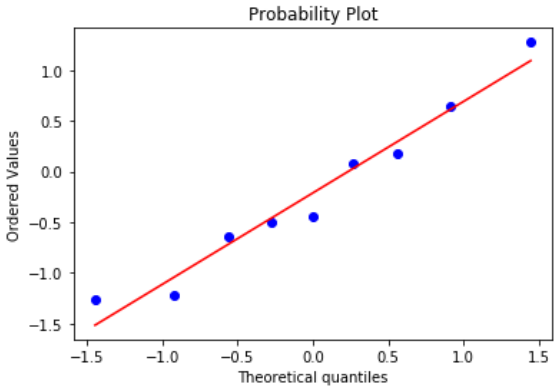
Probability Plot
Ordered Values
Theoretical quantiles

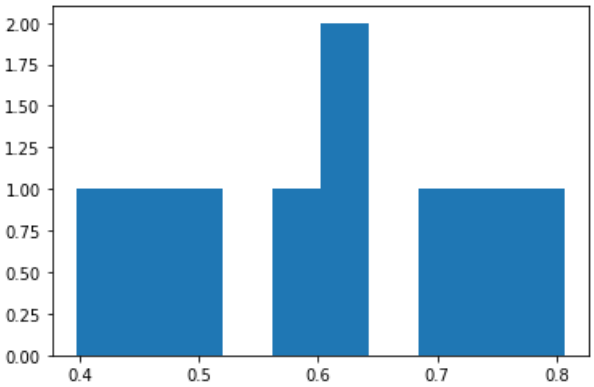

(g)

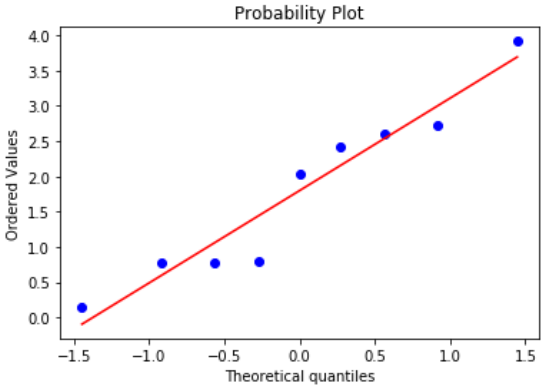

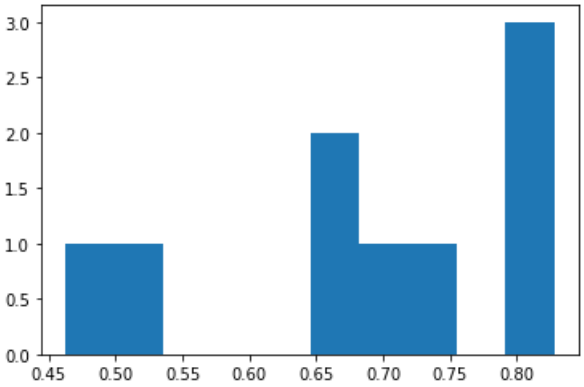

(h)

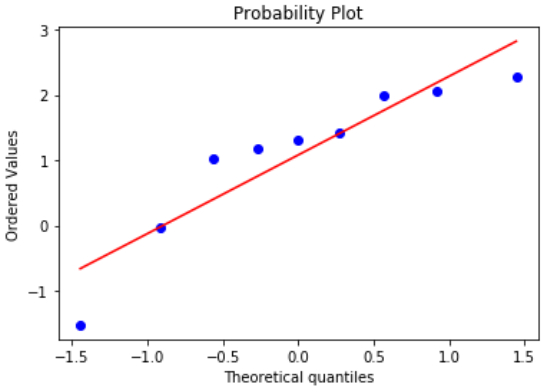

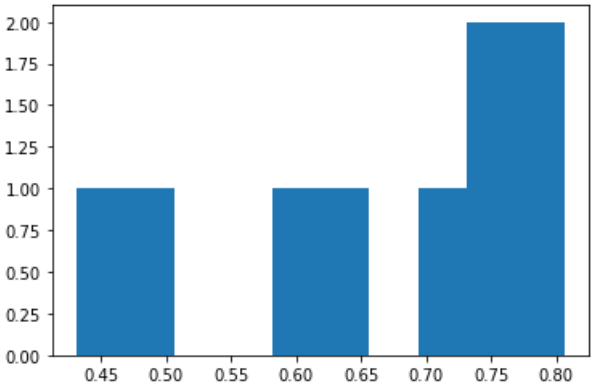

APPENDIX IX - Visual representations of normality displayed as Q-Q plots and histograms to visualise distribution for Autotrophs/(Autotrophs + Heterotrophic Bacteria for; (a) glucose; (b) glucose and turbulence; (c) glucose and silicate; (d) glucose, silicate and turbulence; (e) control; (f) turbulence; (g) silicate; (h) silicate and turbulence

(a)

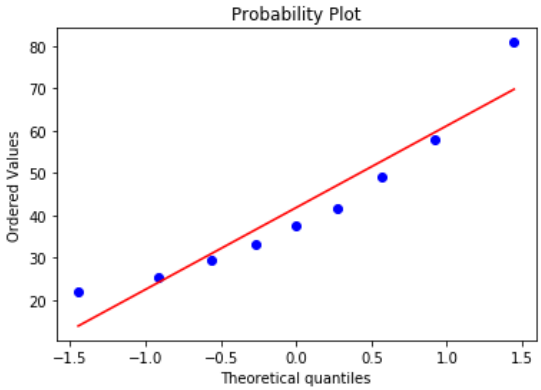
Probability Plot
Ordered Values
Theoretical quantiles

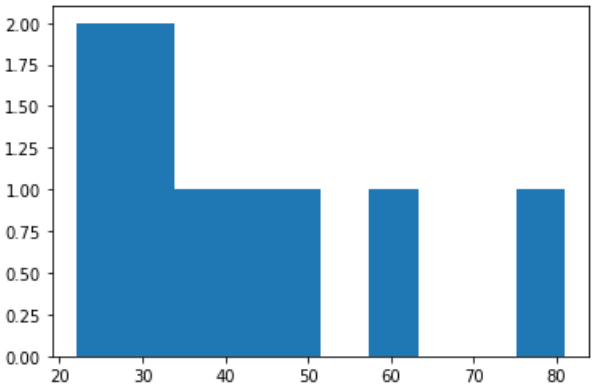

(b)

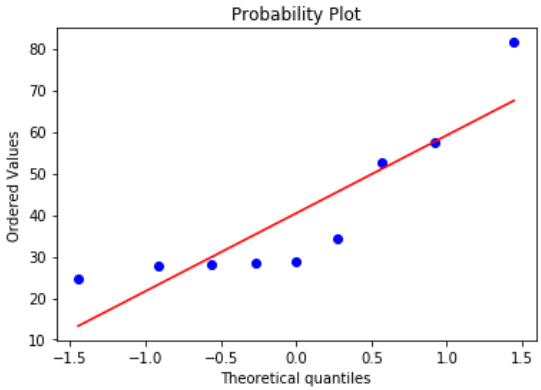
Probability Plot
Ordered Values
Theoretical quantiles

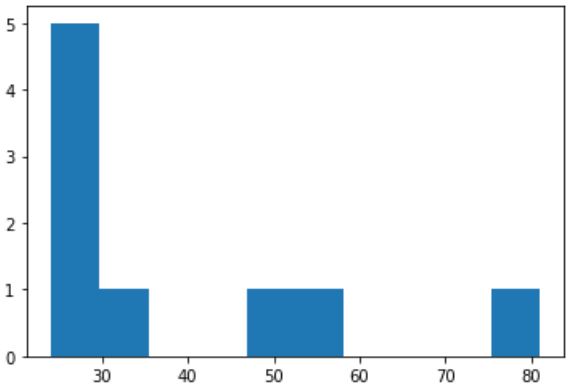

(c)

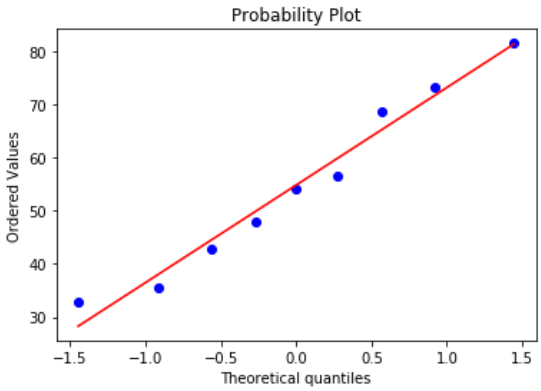
Probability Plot
Ordered Values
Theoretical quantiles

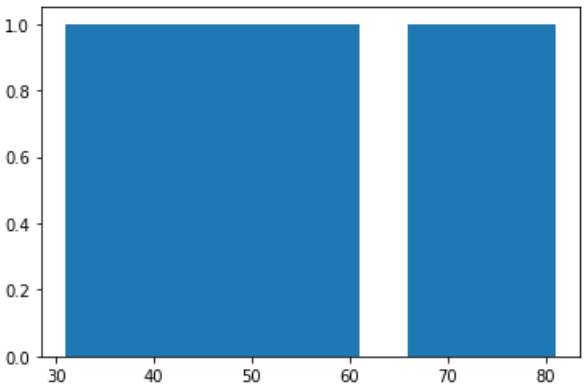

(d)

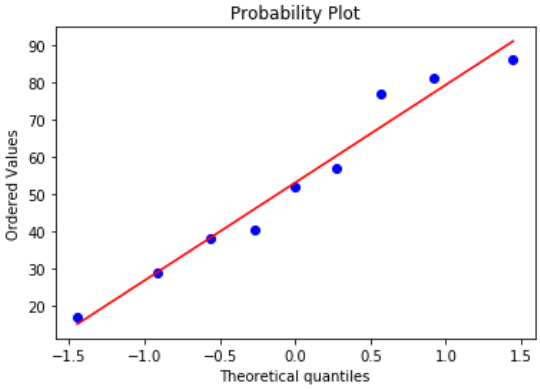
Probability Plot
Ordered Values
Theoretical quantiles

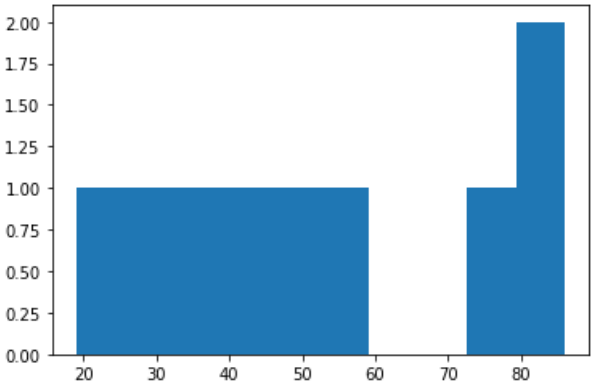

(e)

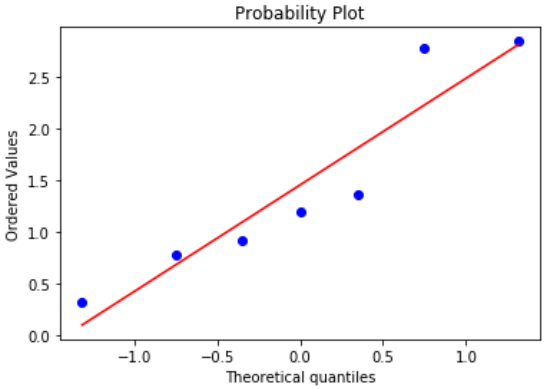
Probability Plot
Ordered Values
Theoretical quantiles

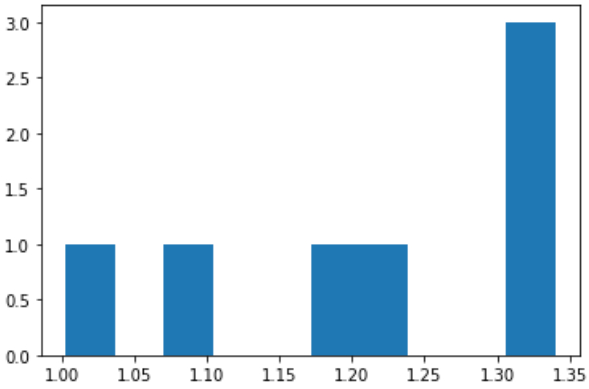

(f)

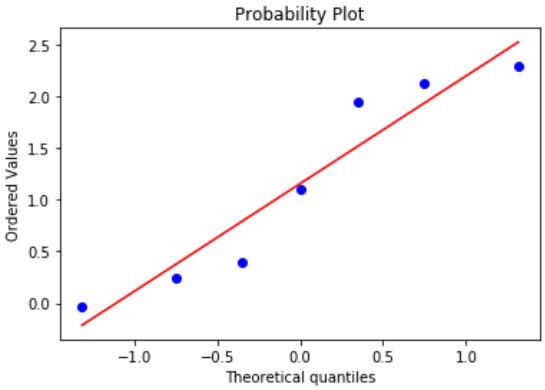
Probability Plot
Ordered Values
Theoretical quantiles

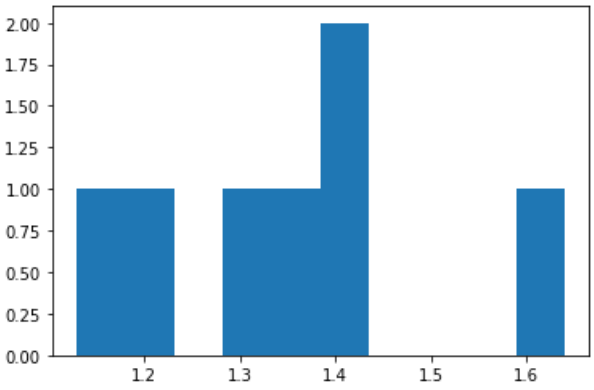

(g)

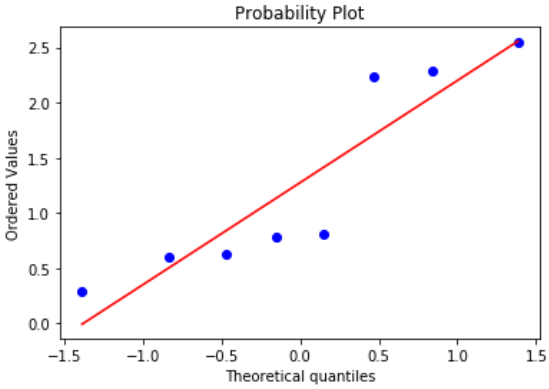

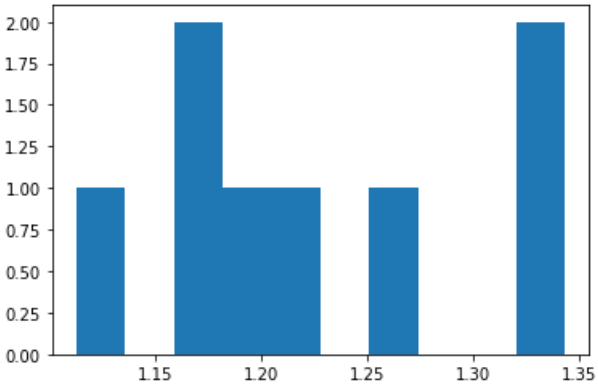

(h)

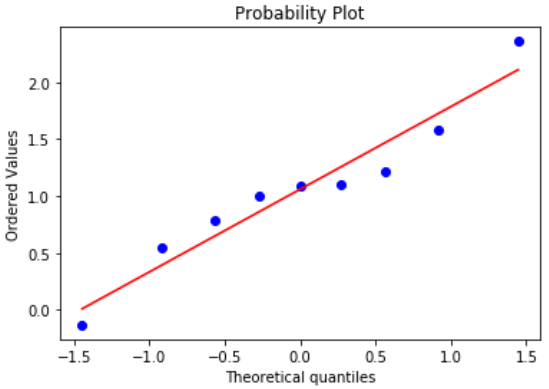

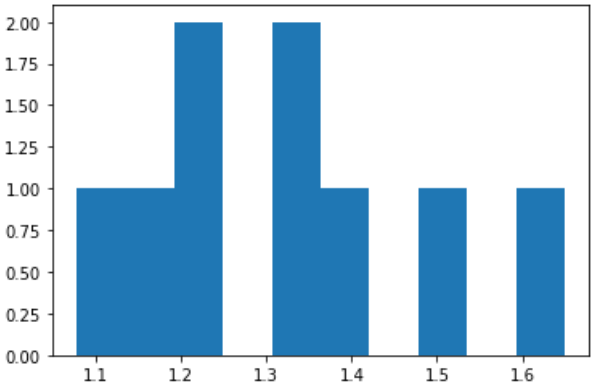

APPENDIX X - Visual representations of normality displayed as Q-Q plots and histograms to visualise distribution for dissolved organic carbon for; (a) glucose; (b) glucose and turbulence; (c) glucose and silicate; (d) glucose, silicate and turbulence; (e) control; (f) turbulence; (g) silicate; (h) silicate and turbulence